On Ion Chemistry and Propagation

by Robert R. Brown, NM7M

On Ion Chemistry and Propagation

by

Robert R. Brown, NM7M

September 2002

Frontpiece:
Thanks to Rita Carney,
Mt. Vernon, WA.

Contents

Preface

This short article is not meant for publication nor for sale. It is being distributed gratis only to a small number people who have a background and interest in propagation. I hope you can find time to read what I have written, the patience to get through parts that may seem "murky" and you'll ponder the conclusions.

As you know, I have written about both HF and low-band propagation. This article is meant to show how ion chemistry, being there all the time, bridges the extremes, from HF to MF and across solar maximum to solar minimum. At best, it is a brief summary of the main of processes involved in establishing the structure of the ionosphere. It does not attempt to give a comprehensive discussion of that subject; rather it gives some of the main ideas and points the reader toward source material for further study.

My own interest in ion chemistry began with the Great Solar Flare Event of February 23, 1956. I was in my laboratory at the University of New Mexico, standing beside my cosmic ray neutron monitor when, at 0356 UTC, the flare erupted and showered the earth with high energy protons, some penetrating the entire atmosphere and reaching ground level even at the magnetic equator. Needless to say, I was astonished when my sleepy monitor, always measuring cosmic ray background rates, seemed to go crazy, with its counting rate increasing by 1,250%! It was AMAZING!

So I shared my observations with other cosmic ray physicists and began to receive data on their observations. Most of it was much like mine, cosmic ray data from locations around the globe, but some very curious observations were included too, like the artificial sunrise on VLF communications circuits when the flare took place. At the time, such ground-level solar proton events occurred about once every seven years or so and high altitude observations were feasible only for a few.

But in early 1959, I received a wonderful paper from Dana K. Bailey, of the Central Radio Propagation Laboratory in Boulder, on the ionospheric aspects of the flare event, even down to the ion chemistry involved. This was all news to me, far from the concerns that I had regarding solar modulation of the galactic cosmic rays, with energies in the BeV range. But it happened I was changing jobs at the time, going to the Berkeley campus of the University of California, and new research directions seemed quite likely.

The resources available to me at Berkeley were far greater than at Albuquerque. So I decided to mount a balloon expedition to

Alaska, flying radiation detectors at 10 gm below the top of the atmosphere. At that atmospheric depth, the cut-off energy for solar protons is about 100 MeV, instead of a Bev at ground level, below 1,000 gm of atmosphere. It was hoped the solar proton event rate would rise accordingly, perhaps smaller events but seen more frequently at ballon altitudes in the high latitudes. My plan was to go to the University of Alaska in July '59, when my teaching obligation was ended for the year. But suddenly, my prospects looked much brighter as the Minnesota group caught an intense event at balloon altitude in May '59.

I was not disappointed; shortly after my arrival in Alaska, the sun produced three proton events and I had data coming out my ears. With Bailey's marvelous article still fresh in mind, a grad student and I took the proton data, used Bailey's methods and tried to compare ionospheric absorption at College, AK with our results, based on calculations using particle spectra from balloon data.

The agreement was poor and the question was whether Bailey's ionospheric parameters were too crude or the balloon data to rough. Little did we know that we were using a poor model of the geomagnetic field in '59, the centered-dipole that admitted too few particles to the atmosphere. Later, in the mid-60s, the magnetosphere came on the scene, with lower cut-off energies, and experiment and theory came closer together.

Those calculations were focused on the D-region, the end of the range of solar protons. As will be seen later, that region has its own special properties, including formation of negative ions. But my next expedition introduced me to auroral events, where electrons create ionization in the E-region. It was clear that Bailey's methods would not apply but I was most fortunate in meeting Fred Rees and George Reid, theorists at the University of Alaska, and by reading their papers, I managed to educate myself with regard to auroral events.

So in the early 60's, I was deep in ionospheric matters although my primary effort was still experimental, flying my radiation detectors on balloons from the ends of the earth - Macquarie Island, south of Tasmania in '61, then Sweden, Norway and Iceland to the mid-60's and Alaska from '68 til '72, when the "Oil-Boom" shut down all balloon work in Alaska. After that, I moved my balloon operations to Greenland and ended them in '80.

But all the time I maintained a very active interest in how ion chemistry would reveal itself during radiation events. So writing this article is not a schoolboy's exercise, just copying words out of a book. As the saying goes, "I've been there, done

that!", even publishing a number of papers on ion chemistry: on the release of atomic oxygen in the D-region during relativistic electron events, the enhancement of atomic nitrogen and nitric oxide during auroral events, on the effect of energetic electron events on the water cluster ion population in the upper D-region, to name a few.

Since retiring in '82, my interests have been propagation and DXing. Of necessity, I had to move up, from the D- and E-regions during my balloon days, to the F-region. That proved to be quite a challenge as, unlike the D- and E-regions, the F-region is not under solar control, depending just on the solar zenith angle; indeed, ion chemistry plays a much greater role in forming the F-region. But I was prepared for what I encountered.

In giving a brief summary of the main of processes involved in establishing the structure of the ionosphere, it should be quite apparent that sunrise and sunset are complicated events. At sunrise, solar photons do not just rip electrons from atoms and molecules; rather, there's more to it than that, increases in ionization initiating gradual, competing processes which shape the ionosphere in space and time. In short, abundances and rate coefficients determine which ions emerge as prominent and which are submerged as trivial.

It is hoped that the present discussion will convey those ideas and show the reader that there is more to the ionosphere than just a collection of electrons recombining with positive ions of nitrogen and oxygen. So in what follows, there is mention of ion-atom interchanges, negative ions and the role of contaminants in the D-region. In short, it is probably more than you expected. Indeed, it tells us why N_2^+ is not a prominent ion in spite of N_2's abundance, how ozone helps low band DXers and why there are winter anomalies in MUFs and absorption, all due to chemistry.

The other surprise is that ion chemistry is quantitative, with rate coefficients, neutral and ion concentrations used to calculate rates of change in concentrations, even differential equations used to deal with the processes on longer time-scales. In that regard, the reader with mathematical interests would do well by reading Chap. 5 of Brekke's book, listed as a reference. That discussion deals with the mathematics of ionospheric problems and with the aid of numerical methods of solution, a wide range of problems can be explored.

Having said all that, all I can say is "Read on!" I think you'll find it interesting.

Anacortes, WA, September 2002.

Introduction -

Hams understand that DX propagation depends on the presence of an ionosphere overhead, with solar radiation from the sun releasing electrons from atoms and molecules in the atmosphere. Part of that process is solar physics, dealing with the number and energy of photons in each part of the the solar spectrum; the other part is ion chemistry, how the electrons, ions, atoms and molecules interact with each other to produce a propagation medium. That medium is there, from HF to MF, from solar maximum to solar minimum.

The last process is our concern, not the physics of signal refraction and absorption along paths. You can find the results of such matters in various propagation programs; we're going to look at how the ionosphere is formed as the sun rises, decays at night and changes when solar disturbances occur.

The Atmosphere -

The atmosphere consists mainly of nitrogen (78%) and oxygen (20%) molecules and is held close by the earth's gravitational field. There are other minor constituents (water vapor and carbon dioxide) in the lower regions as well as pollutants (nitric oxide, carbon monoxide) from human and industrial activity. The lower atmosphere is well-mixed below 100 km by the turbulence of its weather systems but it gradually separates by atomic and molecular weight above that height due photo-dissociation by solar photons.

The atmosphere is exposed to the radiation from the sun, from the far infra-red (>10,000 Angstroms) to short wavelengths in the Xray range (<1 Angstrom). The energy input to the atmosphere is 1,380 W/m^2, the "Solar Constant", largely in the visible portion of the spectrum.

Energetic solar radiation does penetrate below the 100 km level and begins to dissociate the nitrogen and oxygen molecules as well as minor constituents:

$$N_2 + \text{photon} \text{ -----> } N + N$$
$$O_2 + \text{photon} \text{ -----> } O + O$$
$$H_2O + \text{photon} \text{ ----> } O + OH$$

Atomic nitrogen does little but recombine to reform as diatomic molecules again by a radiative process but atomic oxygen is a very active species, in a chemical sense, and enters into an important chemical cycle with ozone, both day and night:

$O_2 + h\nu$ (<2423 A) -----> O + O O_2 dissociation
$O_3 + h\nu$ (<11,000 A)-----> O_2 + O O_3 dissociation
O + O + M -----> O_2 + M three-body recombination
O + O_2 + M -----> O_3 + M three-body association
O + O_3 -----> O_2 + O_2 collisional dissociation

in the daytime and

O + O + M -----> O_2 + M three-body recombination
O + O_2 + M -----> O_3 + M three-body associa3tion
O + O_3 -----> O_2 + O_2 collisional dissociation

at night.

Those chemical reactions are just like the ones studied in high school chemistry except they take place in a natural setting, the atmosphere, not in the laboratory. But they are important to us as the ozone in the atmosphere shields us, by absorption, from the harmful effects of solar UV.

In that regard, recent global studies have suggested the ozone layer is now decreasing in content, particularly in the polar regions. That has raised the question as to how it could happen, permanently destroying ozone when the oxygen cycle is one which continuously renews itself, cycling between O_2 and O_3. The present ideas are that catalytic cycles also take place in the atmosphere which destroy ozone by converting it over into oxygen molecules, O_2, in a one-way process, with the catalyst remaining after a cycle is completed.

Perhaps the most elementary catalytic cycles originate with fragments from water vapor, H and OH, dissociated by solar UV:

H + O_3 ----->OH + O_2
OH + O -----> H + O_2

which is equivalent to O_3 + O -----> $2O_2$, with H remaining, and

OH + O_3 -----> HO_2 + O_2
HO_2 + O_3 -----OH + $2O_2$

or

OH + O_3 -----> HO_2 + O_2
HO_2 + O ----->OH + O_2

which are equivalent to $2O_3$ ----->$3O_2$ and O_3 + O -----> $2O_2$, with OH remaining after the cycles.

At the present time, ozone depletion is being examined in

connection with the presence of chlorine and CFC gases in the atmosphere. This is a rapidly moving area of research and for hams, it is best followed in issues of the Scientific American.

It should be noted that ozone molecules, being electrically neutral, do not take part directly in forming the ionosphere. In addition, they are distributed at low altitudes, below 50 km and peaking at about 25 km, while most ionospheric propagation is at higher altitudes. However, they do play an important role by shielding the lower D-region from solar UV around sunrise. That will be treated more fully later in the discussion.

As noted above, atmospheric ozone absorbs solar UV at low angles of incidence on the ionosphere, shielding the lower D-region from solar UV at sunrise. But ozone absorbs solar radiation at other angles of incidence as well and contributes to the heating of the atmosphere and its temperaturee profile. In that regard, the ozone distribution and the average temperature profile are shown in **Figure 1:**

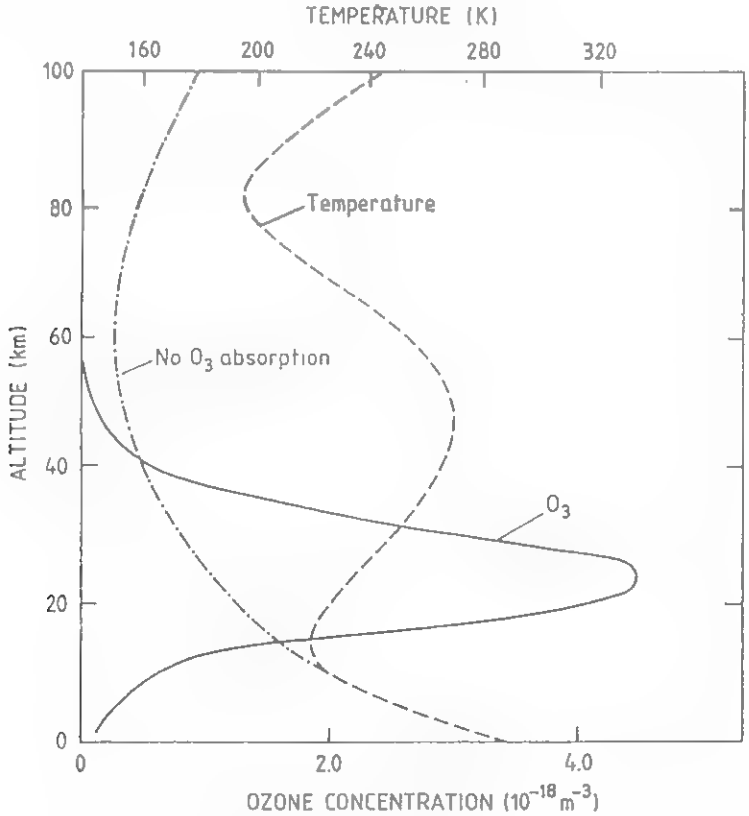

Figure 1 - Ozone concentration below 100 km and average temperature in the region, as well as temperature profile expected in the absence of absorption of solar radiation by ozone.

As would be expected, with the ozone layer lying in a region where the atmospheric temperature varies, there are questions as to how elements of the oxygen-ozone cycle are affected by such variations in temperature. Those are determined by experiment, coefficients for each reaction giving a measure of the rate of the reaction.

For example, consider the simplest reaction,

$$O + O_3 \text{ -----> } O_2 + O_2$$

If an O atom encounters an O_3 molecule, there is a probability b_r per second that the reaction will take place between the two. If the O atom encounters $N(O_3)$ molecules in a cubic meter, the chance of a reaction by the O atom is increased accordingly, to $b_r*N(O_3)$ per second, given that it is moving in a random, chaotic manner and colliding freely with the O_3 molecules in the volume. Finally, if there are N(O) atoms in the cubic meter, along with $N(O_3)$ molecules, the number of reactions per second, destroying O_3 by a reaction with O, in a cubic meter is given by:

$$b_r*N(O)*N(O_3)$$

If one goes to the current literature, the value for br is found to be:

$$3.3E\text{-}17*\exp(-2115/T) \text{ m}^3/\text{sec}.$$

where T is the Kelvin temperature.

On the other hand, the three-body recombination of O atoms,

$$O + O + M \text{ -----> } O_2 + M$$

shown shows no apparent temperature dependence in its reaction rate coefficient

$$2.7E\text{-}45 \text{ m}^6/\text{sec}$$

while the three-body association reaction that creates O3

$$O + O_2 + M \text{ ----> } O_3 + M$$

shows a somewhat different reaction rate dependence

$$5.8E\text{-}47*\exp(+448/T) \text{ m}^6/\text{sec}$$

To illustrate the matter, between the temperature extremes in

Figure 1, 190 K and 270 K, the negative exponential for the first reaction varies from 1.5E-05 to 4.1E-04, an increase of 26.7 times, while the positive exponential for the third reaction varies from 10.6 to 5.3, a decrease of 2.0 times. Clearly, those reactions are sensitive to temperature through the thermal motions of the reactants.

The Lower Ionosphere -

The part of the solar spectrum which creates the ionosphere is the same as that which affects and structures the neutral atmosphere. That is shown clearly in Table 1 which summarizes the wavelength and energy thresholds for photo-dissociation and photo- ionization of the principal atmospheric constituents.

	Photo-dissociation Threshold	Energy		Photo-ionization Threshold	Energy
N_2	< 796 A	>15.58 eV	N_2	< 1270 A	> 9.76 eV
O_2	< 2422 A	> 5.12 eV	O_2	< 1026 A	>12.08 eV
NO	< 1905 A	> 6.51 eV	NO	< 1340 A	> 9.25 eV
			O	< 911 A	>13.61 eV

By comparison, the atmosphere is lower, denser and more mechanical in its wave motions than the ionosphere. Both the atmosphere and the ionosphere propagate a wide range of wave frequencies when it comes to wave motions and show dispersive properties. But the sources of wave motion in the atmosphere are more natural than in the ionosphere as artificial wave sources, RF transmitters, abound when it comes to the ionosphere.

Wave propagation in the ionosphere depends on the presence of free electrons and those originate with photo-ionization of atmospheric constituents:

$$N_2 + \text{photon} \text{ -----> } N_2^+ + e^-$$
$$O_2 + \text{photon} \text{ -----> } O_2^+ + e^-$$
$$NO + \text{photon} \text{ -----> } NO^+ + e^-$$
$$O + \text{photon} \text{ -----> } O^+ + e^-$$

Most of the photo-ionizations are near the photo-threshold so the electrons, when freed, have little excess kinetic energy and do not travel far; instead, they are held locally and spiral around geomagnetic field lines.

That aspect may be seen in **Figure 2**, a global map of the critical frequencies foF2 of the F-region. The particular map

is for near solar minimum, with a SSN of 12 and 0600 UTC at an equinox when the sun is over the geographic equator at 90 E longitude. While the earth is symmetrically illuminated at an equinox, the map shows how the F-region is shifted to the north, indicating the ionosphere is under geomagnetic, not solar control.

Now the lower ionosphere, derived from various atmospheric constituents, shares in the thermal structure of the atmosphere as the major neutral and ionized elements are of comparable mass and collide at very high rates, above a MHz. So equipartition of energy results in common neutral, electron and ion temperatures, going through maxima and minima in the first 100 km, in **Figure** 1, and in large part relatively independent of solar activity.

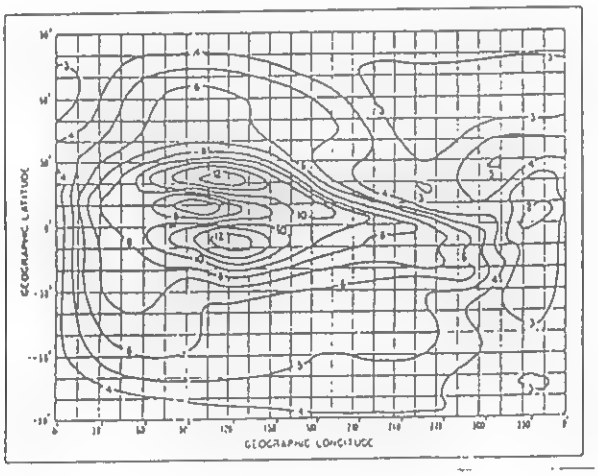

Figure 2 - Global map for foF2 at 0600 UTC in March 1976.

Thus, in a sense, the ionosphere floats or is suspended in the atmosphere, with electrons and positive ions outnumbered by a million to one or more by the neutral constituents. Since most positive ions have the same mass as neutrals and collide with them at a high rate, they follow the motions of the neutrals too, thus being swept along with those motions and electrons following by Coulomb attraction to maintain charge neutrality.

That is a part of ionospheric physics just now appreciated, meteorological fluctuations that have to be added to the layer

distribution of ionization from equilibrium calculations based on steady solar illumination. It should be an important matter in the future but will require making wind measurements at altitudes currently not available on a routine basis.

To go on, once formed, electrons and positive ions can recombine

$$N_2^+ + e^- \xrightarrow{a_1} N + N$$
$$O_2^+ + e^- \xrightarrow{a_2} O + O$$
$$NO^+ + e^- \xrightarrow{a_3} N + O$$
$$O^+ + e^- \xrightarrow{a_4} O + h\nu$$

but that depends on reaction rates and other possibilities due to interactions with the neutral atmosphere. The recombination rates are interesting in that they depend on the electron temperature:

$$N_2^+ + e^- \xrightarrow{a_1} N + N \qquad a_1 = 2.1E\text{-}13*(T_e/300)^{(-.85)}$$
$$O_2^+ + e^- \xrightarrow{a_2} O + O \qquad a_2 = 1.9E\text{-}13*(T_e/300)^{(-.5)}$$
$$NO^+ + e^- \xrightarrow{a_3} N + O \qquad a_3 = 1.8E\text{-}13*(T_e/300)^{(-.39)}$$
$$O^+ + e^- \xrightarrow{a_4} O + h\nu \qquad a_4 = 7.8E\text{-}14*(T_e/300)^{(-.5)}$$

where the a's are in m^3/sec. Of particular note is the slow radiative recombination of O^+. Similar slow recombination is also found with meteoric debris in Sporadic-E layers.

Rearrangement -

Other reactions are possible too and they can the involve the rearrangement of available positive ions, transfer of charge or ion-atom interchange among the major ions:

$$N_2^+ + O_2 \xrightarrow{b_1} O_2^+ + N_2$$
$$N_2^+ + O \xrightarrow{b_2} NO^+ + N$$
$$O_2^+ + N_2 \xrightarrow{b_3} NO^+ + NO$$
$$O^+ + NO \xrightarrow{b_4} NO^+ + O_2$$
$$O^+ + N_2 \xrightarrow{b_5} NO^+ + N$$
$$O^+ + O_2 \xrightarrow{b_6} O_2^+ + O$$

For example, experiment shows that N_2^+ is not one of the prominent ions in the lower ionosphere. That is interesting as the atmospheric data shows N_2 molecules are the most abundant neutrals (78%) in the region. So, that N_2^+ is only a minor ion indicates the N_2^+ created by photo-ionization is rapidly converted over to another ion, O_2^+:

$$N_2^+ + O_2 \xrightarrow{b_1} O_2^+ + N_2 \qquad b_1 = 5E+17*(T_r/300)^{(-.44)}$$

That, in turn, can be converted to NO^+,

$$O_2^+ + N_2 \text{ --}b_3\text{--> } NO^+ + NO$$

The reaction rates of such equations, when combined with neutral and ion densities, determine the rate of rearrangement. As an example, take the last two rearrangement reactions

$$O^+ + N_2 \text{ --}b_5\text{--> } NO^+ + N$$
$$O^+ + O_2 \text{ --}b_6\text{--> } O_2^+ + O$$

The reaction rates are

$$b_5 = 2.1E\text{-}18$$
$$b_6 = 2E\text{-}17*(Tr/300)\text{^}(-.4)$$

in the same units as the recombination reactions. Now the rate of conversion of O^+ to NO^+ is given by

$$b_5*N(O^+)*N(N_2)$$

while the rate of conversion of O^+ to O_2^+ is given by

$$b_6*N(O^+)*N(O_2)$$

So there is a branching ratio for the rearrangement of O^+ to NO^+ or O_2^+,

$$(b_5/b_6)*((N_2)/N(O_2))$$

Similarly, the branching ratio for the rearrangement of N_2^+ to O_2^+ or NO^+ is

$$(b_1/b_2)*((O_2)/N(O))$$

For the third and fourth reactions, the ionic product is the same for both reactions, NO^+, but there is a difference, the reaction of O_2^+ with N_2 creates NO, a trace constituent. While N2 would seem more abundant than NO, the reaction rates show that the N_2 reaction dominates rearrangement of O_2^+ if $N(N_2)>N(NO)$ by a factor of 1E+06:

$$Nr(NO/O_2) = (b_3/b_4)*((N_2)/(NO))$$

or

$$Nr(NO/O_2) = (5E\text{-}22/4.4E\text{-}16)*((N_2)/(NO))$$

or

$$Nr(NO/O_2) = 1.1E\text{-}06*((N_2)/(NO))$$

In the expression for reaction rate b_6, T_r is the average of the ion and neutral temperatures, $(T_i + T_n)/2$. In addition to the

reaction involving b_6, the first two rearrangement reactions with b1 and b2 show similar temperature dependences.

Ionospheric and Atmospheric Databases -

The electron and ion densities used in present calculations are taken from the 1990 version of the International Reference Ionosphere. That provides data for average, quiet conditions. It should be noted, however, there is a more recent version of IRI, released by NASA in 2001. There are differences in the two versions but not significant for our purposes.

The main advantage of IRI90 is that, in giving data in a tabular output, it has a better legend at the bottom of its tables, clearly labeling the date, time (LT and UT), lat and long of the location as well as the SSN. IRI2001 is much poorer in that regard and burdens the user with re-entering all the details of identification and other features. It will not be used here but if any differences exist between IRI90 and IRI2001, they will be noted.

The MSIS program (1986) is used here for atmospheric data from 60 km to 350 km, including O, N2 and O2 number densities as well as mass density and neutral temperature, TN. It is based on satellite and rocket observations and is sensitive to magnetic activity, Ap, as well as solar activity, the 10.7 cm solar flux.

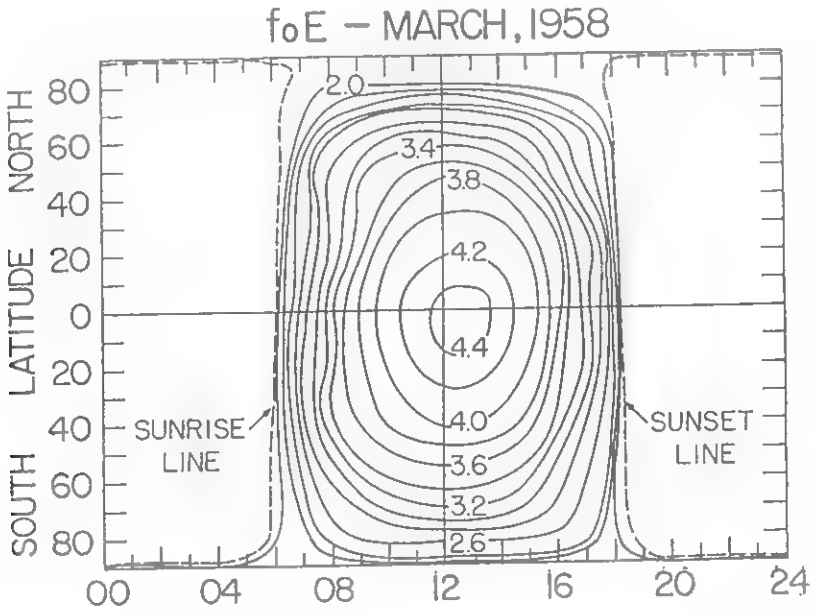

Figure 3 - foE contours around the sub-solar point, for the spring equinox at local noon.

The ionospheric database was established as a result of decades of ionospheric sounding. Earlier, **Figure 2** showed how the electrons at the peak of the F-region were distributed globally but held locally by the geomagnetic field and present in numbers which are controlled by the phase of the solar cycle. At lower altitudes, at the peak of the E-region, ionospheric electrons are largely distributed over the sunlit hemisphere of the earth, as shown by the global map of critical frequencies foE in **Figure 3**, above.

Beyond the question of geomagnetic control, distribution of F-region ionization in **Figure 2** shows that electron densities persist into the hours of darkness, beyond the sunset terminator at 180 E longitude. That is not seen in **Figure 3**, foE critical frequencies comparable to those found around the sub-solar point at 90 deg east longitude are not evident in hours of darkness.

But that is not to say that electron densities vanish in darkness. Of course, the databases show non-vanishing electron densities up to the night-time F-peak but also an electron density valley just above the the E-region, as in **Figure 4**. That proves to be of great value to low-band DXers as their signals may become trapped in the valley and ducted for great distances without lossy ground reflections.

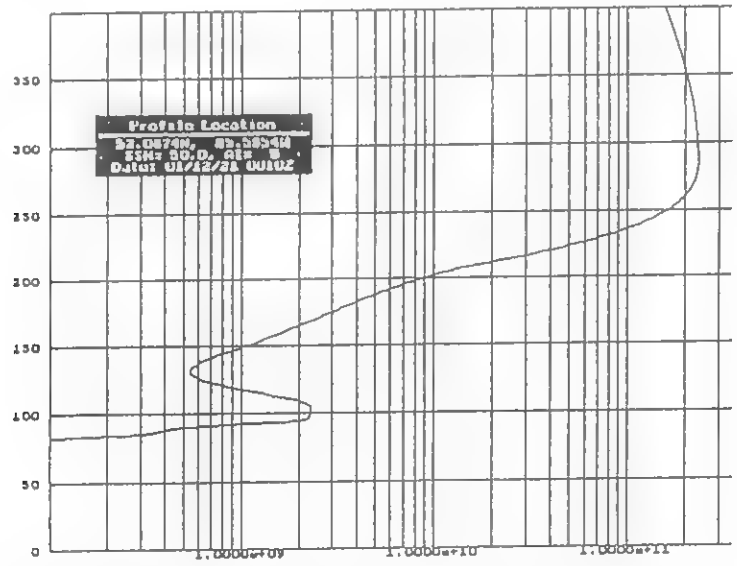

Figure 4 - Night-time electron density profile at 52N, 85W for the winter solstice at 0000 UTC.

Negative Ions -

While the electron density valley shows an unusual feature of electron density distribution, there is another unusual aspect of electron interactions in the lower ionosphere - the formation of negative ions at low altitudes in the D-region. Thus, the participants in the oxygen cycle show an electron affinity and readily form negative ions, O^-, O_2^- and O_3^-, massive in comparison to electrons:

$$O + e^- \xrightarrow{g_1} O^- + h\nu$$
$$O_2 + e^- \xrightarrow{g_2} O^- + O$$
$$O_3 + e^- \xrightarrow{g_3} O^- + O_2$$
$$O_2 + e^- + M \xrightarrow{g_4} O_2^- + M$$
$$O_3 + e^- + M \xrightarrow{g_5} O_3^- + M$$

In contrast to that, the most abundant species, N_2, does not form negative ions and, as noted later, O^- is not found above the D-region .

The formation of negative ions in the D-region at night removes free electrons which would otherwise contribute to the absorption of signals which transit the region. This has been discussed many times and need not be repeated here, except to give the result, shown in **Figure 5**. That result shows how the relative absorption on a per-electron basis varies with band and altitude in the lower ionosphere, where electron-neutral collisions are most frequent.

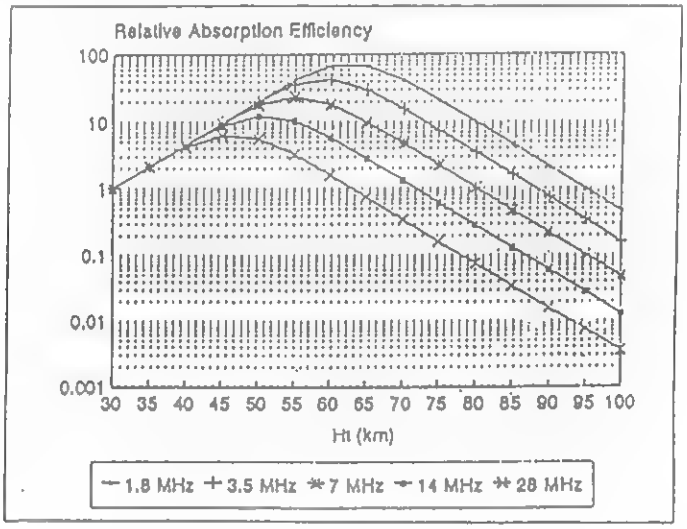

Figure 5 - Relative absorption efficiency per electron

Clearly, absorption is greatest on 160 meters and least on 10 meters and negative ion formation, removing free electrons, is in favor of low-band DXers.

But there are competing processes involving negative ions, with some collisional detachment of electrons at night:

$$O^- + O \xrightarrow{d_1} O_2 + e^-$$
$$O_2^- + O \xrightarrow{d_2} O_3 + e^-$$
$$O_2^- + M \xrightarrow{d_3} O_2 + M + e^-,$$

where M is O_2 or N_2. O- is not found in the E-region, because of the abundance of atomic oxygen O and collisional detachment by the first reaction.

In addition, charge-transfer reactions may take place:

$$O_2^- + O_3 \xrightarrow{t_1} O_3^- + O_2$$
$$O_3^- + O \xrightarrow{t_2} O_2 + O_2$$

as well as ion-ion recombination:

$$O_3^+ + O_2^- \xrightarrow{r_1} O_2 + O_2$$
$$O_2^+ + O_2^- + M \xrightarrow{r_2} O_2 + O_2 + M$$

When the sun rises, electron photo-detachment ensues, freeing electrons, so absorption then returns to day-time levels:

$$O^- + h\nu \xrightarrow{p_1} O + e^-$$
$$O_2^- + h\nu \xrightarrow{p_2} O_2 + e^-$$
$$O_3^- + h\nu \xrightarrow{p_3} O_3 + e^-$$

where the photon energy inm visible radiation should be enough to overcome the electron affinity, e.g., 0.44 eV for O_2-. But experience is otherwise.

Negative ion chemistry is important to propagation across the mid-latitudes, reducing D-region absorption with a sudden drop-off in electron density **(Brekke, 1997)** as negative ion-electron ratios rise to values like 10-100 at night. And the effects of negative ion formation are also seen at night in the polar regions during solar proton events.

During those events, energetic protons from solar flares penetrate deep in the D-region, producing intense ionization and absorption where the electron-neutral collisions are the greatest. But before dawn, negative ion formation may be so great

as to reduce the additional absorption by factors of 4-5.

With dawn, the negative ions in the D-region should start to release electrons by photo-detachment when solar photons reach those altitudes. If O_2- were the principal negative ion, with an electron affinity of 0.44 eV, photons in the visible part of the solar spectrum should start photo-detachment as soon as sunlight reaches the region.

But the electrons prove to be bound so tightly **(Reid, 1976)** as to suggest UV photons are needed for the process. That delays photo-detachment of electrons from negative ions until the solar UV photons pass over the ozone layer, at about 40 km altitude. Low-band DXers depend heavily on propagation near dawn so they get a "bump", a delay of 15-30 minutes in the onset of absorption at sunrise. The model of negative ion chemistry that supports the role of UV is shown in **Figure 6.**

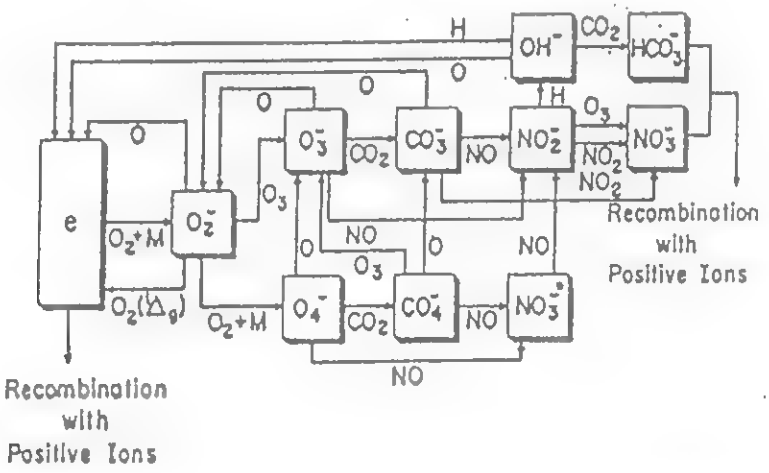

Figure 6 - Negative ion reaction chain during darkness.

It turns out that the minor constituents of the atmosphere and pollutants play a role in negative ion formation. Those differ in their origin, some man-made and others natural. Those of man-made origin are CO_2, NO, NO_2 and can be quite variable in their local concentration and distribution while others, H and H_2O, are of natural origin but still subject to the vagaries of transport by weather systems.

As seen in the diagram, formation of negative ions starts

with O_2- at the left side of the figure and it proceeds toward the right and the final ions, NO_3- and HCO_3-, with which electrons are strongly bound. But given the uncertainties in concentration of the pollutants, some "bottlenecks" may appear along the reaction chain, affecting the rate of advance toward a final negative ion.

Thus, the effects on ionospheric absorption can be quite variable, electrons weakly bound near dusk but firmly bound near dawn. That was not always clear earlier, particularly when it came to solar proton events, and efforts of theorists to use visible radiation to detach electrons at dawn during those events ended in failure.

Clustering -

As indicated in **Figure 6**, the reactions that go to form negative ions involve minor constituents as well as pollutants. It is interesting to note that the terminal ions at the end of the reaction chain could undergo hydration reactions **(Reid, 1976)** with traces of water vapor, leading to the formation of water cluster ions in the form $X-(H_2O)_n$.

That suggestion comes from the fact that positive ions in the quiet D-region show some hydration, with the oxonium ion $H^+(H_2O)$ and its first hydrate found during mass spectrometer measurements on rocket flights. The first reaction is rather direct

$$H_2O^+ + H_2O \text{ -----> } H^+(H_2O) + OH$$

while hydration of O_2^+ involves O_2 in the first step

$$O_2^+ + O_2 + M \text{ -----> } O_4^+ + M$$
$$O_4^+ + H_2O \text{ -----> } O_2^+(H_2O) + O_2$$

The present view with regard to negative ions in the lower ionosphere is that the stable terminal ion is NO_3-, with water molecules loosely attached, formed by similar reactions

$$O_2- + O_2 + M \text{ -----> } O_4- + M$$
$$O_4- + NO \text{ -----> } NO_3- + O_2$$
$$NO_3- + H_2O + M \text{ -----> } NO_3-(H_2O) + M$$

The electron affinity is about 4.5 eV, still requiring UV for any photo-detachment, and aiding low band DXers by the ozone delay in the growth of ionospheric absorption at dawn.

Higher Solar Activity -

While the neutral atmosphere is the constant target of solar photons capable of ionizing its constituents, at the low level of solar activity considered thus far (SSN=12), it is infrequently a target for outbursts of Xrays and solar protons following flare outbursts. The durations of Xray events are short, usually measured in minutes, but can ionize the entire sunlit hemisphere, giving rise to strong absorption of signals until the ionization from the flare outburst recombines with positive ions.

Solar proton events are not frequent at low levels of solar activity but do last longer than Xray bursts, often ionizing the polar caps for days at a time. The rise-time of absorption of signals here at earth depends on the degree of solar activity and the interplanetary field near the flare site, with slow rise-times from sites east of the central meridian of the sun and more rapid ones from the west.

But at higher levels of solar activity, like for the global map in **Figure 7** (SSN=137), solar events are more frequent, more penetrating and of longer duration. So we turn to that level, much like the solar maximum currently in effect during Cycle 23.

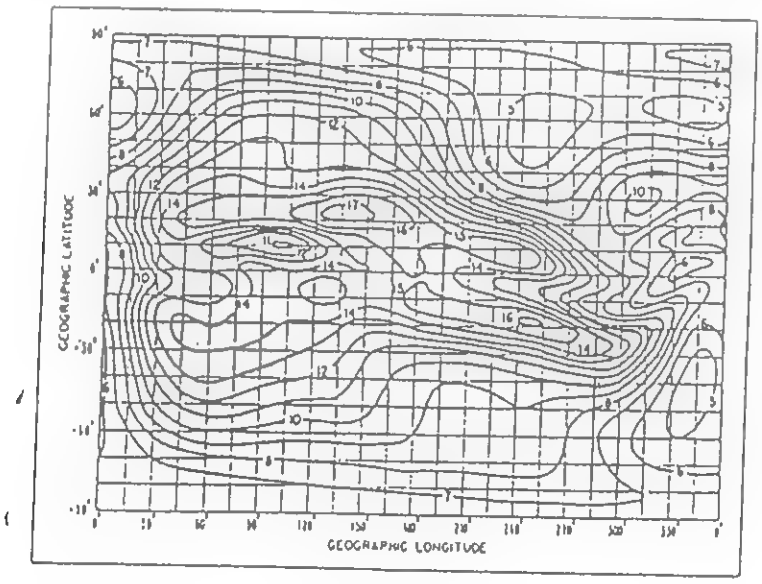

Figure 7 - Global map for foF2 at 0600 UTC in March 1979.

Photo-ionization increases with higher solar activity, along with photo-dissociation. Those are roughly linear variations

with sunspot number, as seen in **Figure 8** below:

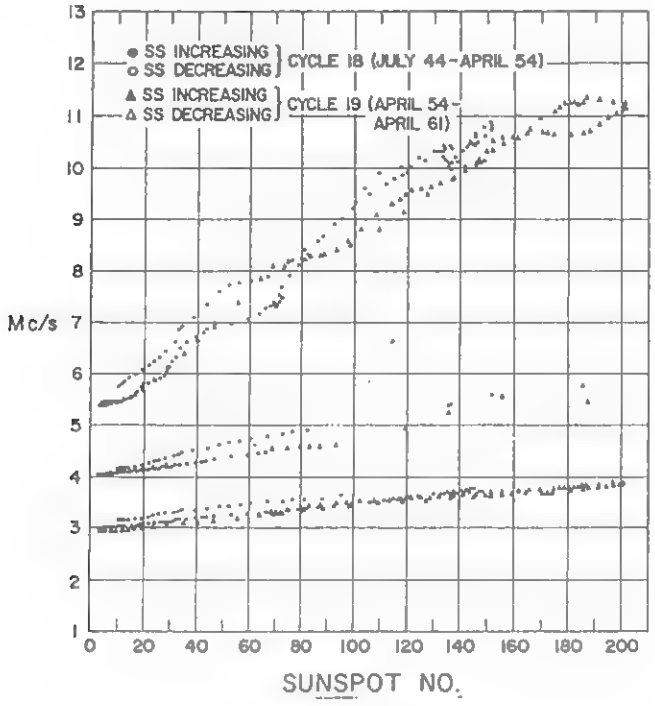

Figure 8 - The variation of critical frequencies (foE, foF1 and foF2) with sunspot number at a mid-latitude site.

From that figure, it is seen the critical frequency foE for the E- layer is more linear than that for the F-region, foF2. Indeed, bending over or the start of saturation of foF2 is evident at high values of sunspot number and that is now confirmed in the recent release of IRI 2001.

Those changes in photo-ionization and photo-dissociation not only change propagation but shift the choice of the operating frequencies used by DXers. So, at low levels of solar activity, the low bands are favored because MUFs are not a problem, there being more than enough ionization overhead at all times. That means low-band signals do not show "skip" in the classical sense and are trapped within the ionosphere when propagated. On the higher bands, however, MUFs are generally too low to permit operating above 14 MHz and that band is often closed at night.

At higher levels of activity, the higher critical frequencies permit oblique propagation to greater distances and DXing on the higher bands. Aside from the changes in magnitude, the ion chemistry at high activity might be expected to be essentially the same as at lower levels. While this may be true of specific ionospheric "anomalies", in MUFs and absorption, it is not true in general, due to changes in temperatures at higher

altitudes.

With regard to MUFs, electron density profiles are developed from ionospheric soundings and make up databases for propagation predictions. In the last analysis, electron density profiles are equilibrium values between the rate of solar ionization and electron recombination. It is of interest to compare critical frequencies, summer/winter, to see changes with seasons.

At a mid-latitude site like Boulder, CO, IRI90 shows the electron density for SSN=12 peaks at about the same altitude at noon in winter, 230 km, as in summer, 240 km. But winter gives 6.8 MHz for foF2 or 5.7E+05 electrons/cm3 at the foF2 peak, greater than of 5.2 MHz or 3.4E+05 electrons/cm3 at 240 km at local noon during summer.

For SSN=137, the electron density peaks at about the same altitude at noon in winter, 280 km, as in summer, 300 km. But winter gives 12.3 MHz for foF2 or 1.9E+06 electrons/cm3, greater than of 7.8 MHz or 7.6E+05 electrons/cm3 at 300 km at local noon during summer. Now those results are clearly anomalous as there is more solar illumination on the F-region at noon in the summer than in the winter!

But the F-region is not under direct solar control like the E-region, mentioned earlier; the E-region shows normal behaviour with foE greater in summer than winter, a foE value of 3.0 MHZ or 1.73E+05 electrons/cm3, at noon in the summer and foE of 2.7 MHz or 9.04E+04 electrons/cm3 for noon in the winter.

Anomalous foF2 behaviour comes from effects of ion-atom interchanges in the neutral atmosphere. For noon in winter, consider a region in the ionosphere, say up at 200 km altitude. The production rate of electrons is due primarily to energetic solar photons (>10 eV) releasing electrons from atomic oxygen, the principal constituent at that altitude. Electrons are lost by recombination with NO^+ and O_2^+ as the recombination process with O^+ is inherently very slow.

But NO^+ results from rearrangement, shown below:

$$O_2^+ + N_2 \text{ -----> } NO^+ + NO$$
$$N_{2+} + O_2 \text{ -----> } NO^+ + NO$$

after production of O_2^+ and N_2^+ solar radiation. So the ratio of electron loss to production really comes down to the ratio of the number of molecules to atoms:

$$(N_2 + O_2)/O$$

and using atmospheric data from the MSIS program for the summer and winter solstices, that summer/winter ratio ranges from 1.5 to 3.5 in going from 100 to 300 km, showing greater loss due to recombination in summer as compared to winter.

With regard to absorption, Appleton and Piggott **(1954)** reported high anomalous absorption on low frequencies in the U.K., during daytime in winter as compared to summer, and from one solar minimum right through to the next solar maximum.

This has been attributed to NO production during long periods of low-level auroral ionization of O_2; for the winter anomaly in absorption, the NO production and loss mechanisms at auroral latitudes include

$$O_2^+ + N_2 \text{ -----> } NO + NO^+$$
$$O_2^- + NO \text{ -----> } O_2 + NO^-$$

the former dominant because of the greater abundance of N_2. With meridional circulation, NO is stable in the dark and accumulates in the polar cap. In that region, NO would then build up and accumulate to form a large, stable reservoir in the polar vortex, meridional motion circulating it around and downward to D-region, heights, then equatorward and upward again.

Those features are summarized by **Garcia et (1987)** and go on to discuss how the vortex is emptied, by equatorward leakage of NO due to brief changes in atmospheric circulation or at the end of winter.

There are differences between the polar caps when it comes to circulation, the southern region being quite smooth and NO stable there until the end of its winter, because of the uniformity of its topography, a large continent surrounded by an ocean. On the other hand, the topography of the northern polar cap is far more varied and there will be equatorward leakage of NO from time to time, bringing NO to lower latitudes. That leakage is a source of more targets for photo-ionization in the winter months and is now considered responsible for the winter anomaly in absorption during day-time hours.

Conclusion -

The ionosphere has its beginning with sunrise, when solar radiation penetrates the upper atmosphere and begins to dissociate the nitrogen and oxygen molecules as well as minor

constituents:

$$N_2 + \text{photon} \text{ -----> } N + N$$
$$O_2 + \text{photon} \text{ -----> } O + O$$
$$H_2O + \text{photon} \text{ ----> } O + OH$$

While it is clear that in the ionization present during hours of darkness comes from that formed earlier during daytime hours, that persistence is largely due to the low recombination rate of electrons and positive ions by processes as given below:

$$N_2^+ + e^- \text{ -----> } N + N$$
$$O_2^+ + e^- \text{ -----> } O + O$$
$$NO^+ + e^- \text{ -----> } N + O$$
$$O^+ + e^- \text{ -----> } O + \text{photon}$$

In between the rising and setting of the sun, there is an amazing amount of chemistry that takes place between with neutral atoms and molecules in the atmosphere and ion chemistry in the dilute ionosphere.

Under quiet solar/terrestrial conditions, without magnetic or auroral activity, DXing on high bands is relatively predictable, depending on the sunspot count and without surprises. In a sense, atmospheric and ionic chemistry are not working against the DXer. Thus, negative ions are formed naturally at night, lowering the number of free electrons that give rise to absorption in the D- region. And the atmospheric ozone layer shields negative ions at low altitude from detachment by solar UV as dawn approaches.

Those circumstances involve ion chemistry going through quasi-equilibrium conditions, almost in a passive manner from dawn to dusk. But that changes when energy inputs to the atmosphere/ionosphere take place. Then atmospheric and ionic chemistry respond, perhaps changing the environment where the input takes place to the advantage/disadvantage of the DXer, depending on the band.

Given the above remarks, DXers would do well to log the daily values of solar/terrestrial indices **(Luetzelschwab, 2002)** from WWV broadcasts to determine times of high solar activity, for their HF operations, and times of low geomagnetic activity for low-band operations. That done, ion chemistry will be working to their advantage all the time.

Conclusion -

An example is the change in the general ionospheric electron density that follows with an increase in solar activity - that increases the ionospheric absorption on low-band signals and requires higher radiation angles to go beyond the E-layer for long hops while it raises MUFs and the height of the F-layer, to the advantage of HF DXers. The low-band DXer loses while the HF DXer gains in the process.

There are no advantages to events where the energy input is delivered to the lower ionosphere - solar Xray bursts, proton events or the penetrating electron (REP) events. The electron density is raised above normal levels at low altitudes and absorption increases accordingly. Auroral events affect ionization at high altitudes, say 100 km upward, and if not too intense, they are more curious than anything else, skewing paths and producing fluttery signals. But if the solar wind disturbance is quite intense, a magnetic storm may be involved, with field lines in the magnetosphere disturbed to the point that lowered MUFs as well as signal skewing results from wave reflection or scattering.

Given the above remarks, DXers would do well to log the daily values of solar/terrestrial indices **(Luetzelschwab, 2002)** from WWV broadcasts to determine times of HIGH solar activity, for their HF operations, and times of LOW geomagnetic activity for low-band operations. That done, ion chemistry will be working to their advantage all the time.

Post Script -

But if any low-band DXer is not satisfied with the "hand" that ion chemistry deals on a given day, our DXer might consider what it would be like if the negative ion reaction leading to electron attachment to form O_2^-

$$O_2 + e^- + M \xrightarrow{g_4} O_2^- + M$$

had a smaller rate coefficient, say by an order of magnitude or two, or if the negative ion reaction leading to collisional detachment of electrons from O_2^-

$$O_2^- + M \xrightarrow{d_3} O_2 + M + e^-,$$

had a larger rate coefficient, by an order of magnitude or two. The electron density in the night-time D-region would be far, far greater, with absorption to match and little in the way of DX.

And our HF DXer would do well to ponder the situation if simple theory for the F-region reaction

$$O^+ + N_2 \text{ --}b_5\text{--> } NO^+ + N$$

did not prove inadequate, with laboratory experiment giving a rate coefficient, 2E-18 m^3/sec, about two orders of magnitude smaller at thermal energies than chemical theory predicts. Were that not the case, "F-region ionization would decay as rapidly as E-region decays after sunset since the molecular ions that are formed recombine rapidly. If the F-region ions were to recombine, the electron density would decrease to levels that would be insufficient to reflect radio waves, essentially destroying long- distance radio communication at night." **(Rees, 1989)**

I close with a phrase from Charles Dickens' "Oliver Twist":

"Be grateful, you ungrateful wretch!"

References

Appleton, E.V and R.W. Piggott, J. Atm. Terr. Phys, p. 141, 1954.

Bailey, D.K., Proc IRE, 47, 255, 1959.

Bilitza, D. International Reference Ionosphere (IRI 90), National Space Data Center, Greenbelt, MD, 1990.

Bilitza, D., International Reference Ionosphere, Goddard Space Flight Center, NASA, 2001.

Brekke, A., Physics of the Upper Polar Atmosphere, Wiley-Praxis Series on Atmospheric Physics, 1997.

Brown, R.R., Auroral Enhancement of Atomic Nitrogen, J. Atmosph. Terr. Physics, Vol. 30, pp. 55-61, 1968.

Brown, R.R., On the Influence of Energetic Electron Precipitation on the Water Cluster Ion Population in the Upper D-region, J. Atmosph. Terr. Physics, Vol. 32, 1747, 1970.

Brown, R.R, Atmospheric Ozone - a Sub-Ionospheric Factor in 160 Meter DXing, The Low Band Monitor, November 1998.

Davies, K., Ionospheric Radio, Peter Perigrinus Ltd, London, 1990.

Garcia, R.R., Susan Solomon, Susan K. Avery, and G.C. Reid, Transport of Nitric Oxide and the D-Region Winter Anomaly, J. Geophys. Res., 92, 977, 1987.

Hargreaves, J. K., The Solar-Terrestrial Environment, Cambridge University Press, 1992.

Luetzelschwab, R.C., WWV Format Change, The DX Magazine, July/August 2002.

Rees, M.H., Physics and chemistry of the upper atmosphere, Cambridge University Press, 1989.

Reid, G.C., Ion chemistry in the D-region, Advances in Atomic and Molecular Physics, Vol. 12, p. 375, 1976.

Reid, G.C., Solar Energetic Particles and their Effect on the Terrestrial Environment, Physics of the Sun, Vol. III. pp. 251-278, 1986.

Appendices

The appendices which follow give selected data for the distribution of ions (I-1 to I-8) and neutral species (A-1 to A-8) in the ionosphere and neutral atmosphere. The selection is quite specific: at Boulder, CO (40N, 105W), for local noon and midnight at the summer and winter solstices and for the two levels of solar activity, SSN=12 and SSN=137, in the text.

The tables of data provide "food for thought" in that they show, among other things, how rearrangement of ions and atoms modifies the ion distribution. Indeed, the nitrogen molecular ion is not present in the tables, even to 1% abundance day or night, due to its rapid reaction with molecular oxygen. And the emergence of atomic oxygen as the major neutral species at high altitudes points to how atomic distributions are controlled by particle speed, the lighter and faster atoms rising to greater heights in the earth's gravitational field.

In any event, the data are worth reviewing and using in numerical examples to see the power of ion chemistry. A good case is to find the N_2^+ concentration at 100 km, say at noon on the winter solstice when SSN = 137:

By I-7, the electron density N_e is 1.18E+11/m^3 and the positive ion density N^+ are the same, by charge neutrality in the volume. So the loss rate of negative charge by electron recombination equals the solar production rate of positive charge by photo-ionization:

$$Q(+) = a_{avs} * N_e * N^+$$

as there is no ion-ion recombination due to photo-detachment of electrons from any negative ions that may be formed. Taking the average electron recombination coefficient as 2E-13 m^3/sec (see p. 7 of text), the solar ionization rate is:

$$Q(+) = (2E-13)*(1.18E+11)^2 = 2.78E+09 \text{ ions/m}^3\text{/sec.}$$

In photo-equilibrium, the production of N_2^+, by abundance, is equal to the loss by electron recombination and ion-atom interchange with oxygen O_2:

$$(.78)*Q(+) = a_1*(N_2^+)*(N_e) + b_1*(N_2^+)*(O_2)$$

or

$$(N_2^+) = [(.78)*Q(+)]/[a_1*(N_e) + b_1*(O_2)]$$

or

$$(N_2^+) = [.78*2.8E+09]/[2E-13*1.2E+11 + 5E-17*2E+18]$$

or

$$(N_2^+) = 2.2E+07 \text{ ions/m}^3$$

which is less than 1% of the electron and total positive ion density at 100 km, as noted earlier.

Date: 06/21, Time 12 L.T., SSN = 12, 40 N, 105 W

H/KM	ELECTRON DENSITY		TEMPERATURES				ION PERCENTAGE DENSITIES				
	NE/CM-3	NE/NMF2	TN/K	TI/K	TE/K	TE/TI	O+	H+	He+	O2+	NO+
60.0	0	-1.0000	-1	-1	-1	-1.00	-1	-1	-1	-1	-1
70.0	251	0.0007	-1	-1	-1	-1.00	-1	-1	-1	-1	-1
80.0	605	0.0018	-1	-1	-1	-1.00	-1	-1	-1	-1	-1
90.0	13664	0.0402	-1	-1	-1	-1.00	-1	-1	-1	-1	-1
100.0	117732	0.3463	-1	-1	-1	-1.00	0	0	0	50	50
110.0	133055	0.3913	-1	-1	-1	-1.00	1	0	0	42	57
120.0	134802	0.3965	352	352	352	1.00	1	0	0	37	62
130.0	153760	0.4522	487	487	490	1.01	2	0	0	34	64
140.0	176454	0.5190	585	585	627	1.07	4	0	0	33	63
150.0	201734	0.5933	656	656	764	1.16	7	0	0	32	61
160.0	226394	0.6658	709	709	902	1.27	10	0	0	31	59
170.0	244749	0.7198	747	747	1039	1.39	14	0	0	30	56
180.0	264717	0.7785	775	775	1176	1.52	17	0	0	29	54
190.0	288594	0.8488	796	796	1313	1.65	20	0	0	27	53
200.0	307911	0.9056	811	811	1450	1.79	23	0	0	21	56
210.0	322388	0.9482	822	829	1583	1.91	28	0	0	13	60
220.0	332168	0.9769	830	846	1710	2.02	32	0	0	7	61
230.0	337749	0.9933	836	864	1833	2.12	38	0	0	4	58
240.0	339900	0.9997	840	882	1956	2.22	45	0	0	2	53
250.0	339250	0.9978	843	900	2079	2.31	53	0	0	1	46
260.0	335483	0.9867	846	918	2201	2.40	62	0	0	1	38
270.0	328775	0.9669	848	936	2323	2.48	72	0	0	0	27
280.0	319433	0.9395	849	954	2445	2.56	84	0	0	0	16
290.0	307834	0.9054	850	972	2561	2.63	95	0	0	0	5
300.0	294394	0.8658	851	990	2650	2.68	99	0	0	0	1
310.0	279548	0.8222	851	1008	2687	2.67	100	0	0	0	0
320.0	263729	0.7756	852	1026	2696	2.63	100	0	0	0	0
330.0	247341	0.7274	852	1044	2700	2.59	100	0	0	0	0
340.0	230754	0.6787	852	1062	2704	2.55	100	0	0	0	0
350.0	214286	0.6302	852	1080	2707	2.51	100	0	0	0	0

I-URSI --B0Gul----------I----------I----------I

LAT/LON= 40.0/***** H= 350.0 RZ12= 12.0 MMDD: 621 LT:12.0 SZA= 16.6

MLA/MLO= 48.9/317.8 DIP= 67.4 F10.7= 72.6 DDD: 172 UT:19.0 SDE= 23.4

Date: 06/21, Time 00 L.T., SSN = 12, 40 N, 105 W

H/KM	ELECTRON DENSITY		TEMPERATURES				ION PERCENTAGE DENSITIES				
	NE/CM-3	NE/NMF2	TN/K	TI/K	TE/K	TE/TI	O+	H+	He+	O2+	NO+
60.0	0	-1.0000	-1	-1	-1	-1.00	-1	-1	-1	-1	-1
70.0	0	-1.0000	-1	-1	-1	-1.00	-1	-1	-1	-1	-1
80.0	1	0.0000	-1	-1	-1	-1.00	-1	-1	-1	-1	-1
90.0	477	0.0033	-1	-1	-1	-1.00	-1	-1	-1	-1	-1
100.0	1735	0.0121	-1	-1	-1	-1.00	0	0	0	6	94
110.0	1420	0.0099	-1	-1	-1	-1.00	0	0	0	11	89
120.0	596	0.0042	341	341	341	1.00	0	0	0	19	81
130.0	353	0.0025	469	469	469	1.00	0	0	0	28	72
140.0	399	0.0028	553	553	553	1.00	0	0	0	32	68
150.0	663	0.0046	608	608	631	1.04	1	0	0	32	67
160.0	1107	0.0077	645	645	679	1.05	2	0	0	31	67
170.0	1761	0.0123	669	669	707	1.06	5	0	0	30	66
180.0	2444	0.0170	685	685	730	1.07	8	0	0	28	64
190.0	3494	0.0243	695	695	752	1.08	11	0	0	26	63
200.0	5253	0.0366	702	702	774	1.10	14	0	0	20	66
210.0	8896	0.0620	707	719	797	1.11	18	0	0	12	70
220.0	19663	0.1370	710	735	819	1.11	22	0	0	7	71
230.0	37885	0.2639	712	752	841	1.12	28	0	0	4	69
240.0	62215	0.4334	714	768	864	1.12	34	0	0	2	64
250.0	88980	0.6198	714	784	886	1.13	42	0	0	1	57
260.0	113219	0.7887	715	801	908	1.13	53	0	0	1	47
270.0	130934	0.9121	715	817	931	1.14	65	0	0	0	35
280.0	140649	0.9798	716	834	953	1.14	80	0	0	0	20
290.0	143535	0.9999	716	850	973	1.15	93	0	0	0	7
300.0	142998	0.9962	716	866	987	1.14	99	0	0	0	1
310.0	141167	0.9834	716	883	987	1.12	100	0	0	0	0
320.0	138152	0.9624	716	899	981	1.09	100	0	0	0	0
330.0	134093	0.9341	716	915	972	1.06	100	0	0	0	0
340.0	129148	0.8997	716	932	964	1.03	100	0	0	0	0
350.0	123496	0.8603	716	948	956	1.01	100	0	0	0	0

I-URSI --B0Gul----------I----------I----------I
LAT/LON= 40.0/***** H= 350.0 RZ12= 12.0 MMDD: 621 LT: 0.0 SZA=116.6
MLA/MLO= 48.9/317.8 DIP= 67.4 F10.7= 72.6 DDD: 172 UT: 7.0 SDE= 23.4

Date: 12/21, Time 12 L.T., SSN = 12, 40 N, 105 W

H/KM	ELECTRON DENSITY		TEMPERATURES				ION PERCENTAGE DENSITIES				
	NE/CM-3	NE/NMF2	TN/K	TI/K	TE/K	TE/TI	O+	H+	He+	O2+	NO+
60.0	0	-1.0000	-1	-1	-1	-1.00	-1	-1	-1	-1	-1
70.0	152	0.0003	-1	-1	-1	-1.00	-1	-1	-1	-1	-1
80.0	378	0.0007	-1	-1	-1	-1.00	-1	-1	-1	-1	-1
90.0	8335	0.0145	-1	-1	-1	-1.00	-1	-1	-1	-1	-1
100.0	80623	0.1406	-1	-1	-1	-1.00	0	0	0	39	61
110.0	90364	0.1576	-1	-1	-1	-1.00	1	0	0	42	57
120.0	91609	0.1598	343	343	343	1.00	1	0	0	46	53
130.0	101305	0.1767	441	441	484	1.10	3	0	0	47	50
140.0	109913	0.1917	514	514	625	1.22	7	0	0	45	48
150.0	120934	0.2109	570	570	766	1.35	15	0	0	39	46
160.0	137249	0.2394	611	611	907	1.48	30	0	0	33	37
170.0	194719	0.3396	643	643	1048	1.63	51	0	0	22	27
180.0	297891	0.5195	667	667	1189	1.78	70	0	0	11	19
190.0	401722	0.7006	685	685	1329	1.94	81	0	0	4	14
200.0	487556	0.8503	698	698	1464	2.10	87	0	0	2	12
210.0	543805	0.9484	709	721	1572	2.18	89	0	0	1	10
220.0	569518	0.9932	716	743	1635	2.20	91	0	0	0	9
230.0	573097	0.9994	722	766	1676	2.19	93	0	0	0	7
240.0	568424	0.9913	727	789	1713	2.17	94	0	0	0	6
250.0	558450	0.9739	730	811	1749	2.16	95	0	0	0	5
260.0	543664	0.9481	733	834	1784	2.14	96	0	0	0	4
270.0	524699	0.9150	735	856	1820	2.13	97	0	0	0	3
280.0	502271	0.8759	736	879	1856	2.11	99	0	0	0	1
290.0	477145	0.8321	738	902	1892	2.10	100	0	0	0	0
300.0	450093	0.7849	738	924	1930	2.09	100	0	0	0	0
310.0	421852	0.7357	739	947	1970	2.08	100	0	0	0	0
320.0	393093	0.6855	740	969	2012	2.08	100	0	0	0	0
330.0	364414	0.6355	740	992	2054	2.07	100	0	0	0	0
340.0	336309	0.5865	740	1015	2096	2.07	100	0	0	0	0
350.0	309177	0.5392	741	1037	2138	2.06	100	0	0	0	0

I-URSI --B0Gul----------I----------I----------I

LAT/LON= 40.0/***** H= 350.0 RZ12= 12.0 MMDD:1221 LT:12.0 SZA= 63.5

MLA/MLO= 48.9/317.8 DIP= 67.4 F10.7= 72.6 DDD: 355 UT:19.0 SDE=-23.5

Date: 12/21, Time 00 L.T., SSN = 12, 40 N, 105 W

H/KM	ELECTRON DENSITY		TEMPERATURES				ION PERCENTAGE DENSITIES				
	NE/CM-3	NE/NMF2	TN/K	TI/K	TE/K	TE/TI	O+	H+	He+	O2+	NO+
60.0	0	-1.0000	-1	-1	-1	-1.00	-1	-1	-1	-1	-1
70.0	0	-1.0000	-1	-1	-1	-1.00	-1	-1	-1	-1	-1
80.0	1	0.0000	-1	-1	-1	-1.00	-1	-1	-1	-1	-1
90.0	472	0.0079	-1	-1	-1	-1.00	-1	-1	-1	-1	-1
100.0	1735	0.0290	-1	-1	-1	-1.00	-1	-1	-1	-1	-1
110.0	1416	0.0237	-1	-1	-1	-1.00	0	0	0	16	84
120.0	586	0.0098	332	332	332	1.00	0	0	0	29	71
130.0	341	0.0057	427	427	427	1.00	0	0	0	38	62
140.0	382	0.0064	494	494	494	1.00	1	0	0	42	58
150.0	637	0.0107	541	541	561	1.04	2	0	0	39	59
160.0	1077	0.0180	575	575	620	1.08	7	0	0	34	59
170.0	1732	0.0290	599	599	672	1.12	20	0	0	29	51
180.0	2099	0.0351	616	616	722	1.17	43	0	0	20	37
190.0	2587	0.0433	629	629	773	1.23	65	0	0	10	25
200.0	3284	0.0550	637	637	823	1.29	78	0	0	4	18
210.0	4427	0.0741	643	651	874	1.34	85	0	0	1	14
220.0	7779	0.1302	648	664	924	1.39	88	0	0	1	11
230.0	15117	0.2530	651	677	974	1.44	90	0	0	0	10
240.0	25041	0.4191	653	690	1025	1.48	92	0	0	0	8
250.0	36117	0.6045	655	704	1075	1.53	94	0	0	0	6
260.0	46319	0.7753	656	717	1126	1.57	95	0	0	0	5
270.0	53943	0.9029	657	730	1176	1.61	97	0	0	0	3
280.0	58278	0.9755	658	744	1226	1.65	98	0	0	0	2
290.0	59713	0.9995	658	757	1274	1.68	99	0	0	0	1
300.0	59576	0.9972	658	770	1310	1.70	100	0	0	0	0
310.0	58917	0.9862	659	783	1326	1.69	100	0	0	0	0
320.0	57794	0.9674	659	797	1329	1.67	100	0	0	0	0
330.0	56256	0.9416	659	810	1331	1.64	100	0	0	0	0
340.0	54363	0.9099	659	823	1332	1.62	100	0	0	0	0
350.0	52181	0.8734	659	836	1334	1.59	100	0	0	0	0

I-URSI --B0Gul----------I----------I----------I

LAT/LON= 40.0/***** H= 350.0 RZ12= 12.0 MMDD:1221 LT: 0.0 SZA=163.5

MLA/MLO= 48.9/317.8 DIP= 67.4 F10.7= 72.6 DDD: 355 UT: 7.0 SDE=-23.5

Date: 06/21, Time 12 L.T., SSN = 137, 40 N, 105 W

H/KM	ELECTRON DENSITY		TEMPERATURES				ION PERCENTAGE DENSITIES				
	NE/CM-3	NE/NMF2	TN/K	TI/K	TE/K	TE/TI	O+	H+	He+	O2+	NO+
60.0	0	-1.0000	-1	-1	-1	-1.00	-1	-1	-1	-1	-1
70.0	640	0.0008	-1	-1	-1	-1.00	-1	-1	-1	-1	-1
80.0	1541	0.0020	-1	-1	-1	-1.00	-1	-1	-1	-1	-1
90.0	31771	0.0417	-1	-1	-1	-1.00	-1	-1	-1	-1	-1
100.0	177067	0.2323	-1	-1	-1	-1.00	0	0	0	61	39
110.0	185897	0.2439	-1	-1	-1	-1.00	1	0	0	48	52
120.0	188339	0.2471	376	376	376	1.00	1	0	0	39	60
130.0	205086	0.2690	555	555	555	1.00	3	0	0	33	64
140.0	225393	0.2957	700	700	700	1.00	6	0	0	30	64
150.0	250839	0.3291	818	818	818	1.00	11	0	0	27	61
160.0	282776	0.3710	913	913	914	1.00	20	0	0	25	55
170.0	320555	0.4205	989	989	1049	1.06	31	0	0	22	47
180.0	359490	0.4716	1052	1052	1183	1.13	41	0	0	19	40
190.0	393922	0.5168	1102	1102	1318	1.20	50	0	0	13	37
200.0	427194	0.5604	1143	1143	1452	1.27	59	0	0	5	36
210.0	481883	0.6322	1176	1176	1583	1.35	68	0	0	2	30
220.0	534232	0.7008	1203	1203	1710	1.42	79	0	0	1	21
230.0	582809	0.7646	1225	1225	1833	1.50	89	0	0	0	11
240.0	626428	0.8218	1242	1242	1956	1.57	97	0	0	0	3
250.0	664212	0.8713	1257	1257	2078	1.65	99	0	0	0	0
260.0	695632	0.9126	1268	1268	2201	1.73	100	0	0	0	0
270.0	720517	0.9452	1278	1278	2323	1.82	100	0	0	0	0
280.0	739028	0.9695	1286	1286	2445	1.90	100	0	0	0	0
290.0	751625	0.9860	1292	1292	2561	1.98	100	0	0	0	0
300.0	759007	0.9957	1297	1297	2650	2.04	100	0	0	0	0
310.0	762057	0.9997	1302	1302	2687	2.06	100	0	0	0	0
320.0	761581	0.9991	1305	1305	2696	2.07	100	0	0	0	0
330.0	757417	0.9936	1308	1308	2700	2.06	100	0	0	0	0
340.0	749640	0.9834	1310	1310	2704	2.06	100	0	0	0	0
350.0	738461	0.9687	1312	1312	2707	2.06	100	0	0	0	0

I-URSI --B0Gul----------I----------I----------I

LAT/LON= 40.0/***** H= 350.0 RZ12=137.0 MMDD: 621 LT:12.0 SZA= 16.6

MLA/MLO= 48.9/317.8 DIP= 67.4 F10.7=180.2 DDD: 172 UT:19.0 SDE= 23.4

Date: 06/21, Time 00 L.T., SSN = 137, 40 N, 105 W

H/KM	ELECTRON DENSITY		TEMPERATURES				ION PERCENTAGE DENSITIES				
	NE/CM-3	NE/NMF2	TN/K	TI/K	TE/K	TE/TI	O+	H+	He+	O2+	NO+
60.0	0	-1.0000	-1	-1	-1	-1.00	-1	-1	-1	-1	-1
70.0	0	-1.0000	-1	-1	-1	-1.00	-1	-1	-1	-1	-1
80.0	1	0.0000	-1	-1	-1	-1.00	-1	-1	-1	-1	-1
90.0	477	0.0010	-1	-1	-1	-1.00	-1	-1	-1	-1	-1
100.0	3715	0.0079	-1	-1	-1	-1.00	0	0	0	6	94
110.0	3057	0.0065	-1	-1	-1	-1.00	0	0	0	11	89
120.0	1284	0.0027	364	364	364	1.00	0	0	0	17	83
130.0	760	0.0016	537	537	537	1.00	0	0	0	25	75
140.0	860	0.0018	667	667	667	1.00	1	0	0	29	70
150.0	1427	0.0030	765	765	782	1.02	2	0	0	30	68
160.0	2383	0.0051	838	838	840	1.00	3	0	0	31	66
170.0	3765	0.0080	893	893	893	1.00	7	0	0	31	63
180.0	4456	0.0095	934	934	934	1.00	12	0	0	28	60
190.0	5326	0.0114	965	965	965	1.00	18	0	0	18	65
200.0	6448	0.0138	989	989	989	1.00	26	0	0	5	68
210.0	7946	0.0170	1006	1006	1006	1.00	38	0	0	1	61
220.0	10064	0.0215	1020	1020	1020	1.00	54	0	0	0	46
230.0	13400	0.0286	1030	1030	1030	1.00	75	0	0	0	25
240.0	20884	0.0445	1037	1037	1037	1.00	93	0	0	0	7
250.0	42040	0.0897	1043	1043	1043	1.00	99	0	0	0	1
260.0	75666	0.1614	1048	1048	1048	1.00	100	0	0	0	0
270.0	122923	0.2622	1051	1051	1051	1.00	100	0	0	0	0
280.0	181996	0.3882	1053	1053	1053	1.00	99	1	0	0	0
290.0	247929	0.5289	1055	1055	1055	1.00	98	2	0	0	0
300.0	313710	0.6692	1057	1057	1057	1.00	96	3	0	0	0
310.0	372178	0.7939	1058	1058	1059	1.00	95	4	0	0	0
320.0	417918	0.8915	1059	1059	1059	1.00	94	5	1	0	0
330.0	448446	0.9566	1059	1059	1059	1.00	93	7	1	0	0
340.0	464375	0.9906	1060	1060	1060	1.00	92	8	1	0	0
350.0	468787	1.0000	1060	1060	1060	1.00	90	9	1	0	0

I-URSI --B0Gul----------I----------I----------I

LAT/LON= 40.0/***** H= 350.0 RZ12=137.0 MMDD: 621 LT: 0.0 SZA=116.6

MLA/MLO= 48.9/317.8 DIP= 67.4 F10.7=180.2 DDD: 172 UT: 7.0 SDE= 23.4

Date: 12/21, Time 12 L.T., SSN = 137, 40 N, 105 W

H/KM	ELECTRON DENSITY		TEMPERATURES				ION PERCENTAGE DENSITIES				
	NE/CM-3	NE/NMF2	TN/K	TI/K	TE/K	TE/TI	O+	H+	He+	O2+	NO+
60.0	0	-1.0000	-1	-1	-1	-1.00	-1	-1	-1	-1	-1
70.0	286	0.0002	-1	-1	-1	-1.00	-1	-1	-1	-1	-1
80.0	710	0.0004	-1	-1	-1	-1.00	-1	-1	-1	-1	-1
90.0	15049	0.0080	-1	-1	-1	-1.00	-1	-1	-1	-1	-1
100.0	117710	0.0627	-1	-1	-1	-1.00	0	0	0	39	61
110.0	126252	0.0672	-1	-1	-1	-1.00	1	0	0	42	57
120.0	127992	0.0681	366	366	366	1.00	1	0	0	46	53
130.0	139446	0.0742	507	507	507	1.00	3	0	0	47	50
140.0	147816	0.0787	621	621	644	1.04	7	0	0	45	48
150.0	157462	0.0838	714	714	782	1.10	15	0	0	39	46
160.0	168886	0.0899	790	790	921	1.17	30	0	0	33	37
170.0	183035	0.0974	851	851	1059	1.24	51	0	0	22	27
180.0	202167	0.1076	902	902	1198	1.33	70	0	0	11	19
190.0	236988	0.1262	943	943	1336	1.42	81	0	0	4	14
200.0	398659	0.2122	977	977	1468	1.50	87	0	0	2	12
210.0	627728	0.3341	1005	1005	1575	1.57	89	0	0	1	10
220.0	897576	0.4778	1027	1027	1637	1.59	91	0	0	0	9
230.0	1178385	0.6273	1046	1046	1678	1.60	93	0	0	0	7
240.0	1436060	0.7644	1061	1061	1714	1.62	94	0	0	0	6
250.0	1642433	0.8743	1073	1073	1750	1.63	95	0	0	0	5
260.0	1782582	0.9489	1083	1083	1785	1.65	96	0	0	0	4
270.0	1856919	0.9885	1092	1092	1821	1.67	97	0	0	0	3
280.0	1878551	1.0000	1099	1099	1856	1.69	99	0	0	0	1
290.0	1873808	0.9974	1104	1104	1892	1.71	100	0	0	0	0
300.0	1858486	0.9893	1109	1109	1930	1.74	100	0	0	0	0
310.0	1833134	0.9758	1113	1113	1970	1.77	100	0	0	0	0
320.0	1798483	0.9574	1116	1116	2012	1.80	100	0	0	0	0
330.0	1755453	0.9344	1119	1119	2054	1.84	100	0	0	0	0
340.0	1705109	0.9076	1121	1124	2096	1.86	100	0	0	0	0
350.0	1648605	0.8776	1122	1135	2138	1.88	100	0	0	0	0

I-URSI --B0Gul----------I----------I----------I

LAT/LON= 40.0/***** H= 350.0 RZ12=137.0 MMDD:1221 LT:12.0 SZA= 63.5

MLA/MLO= 48.9/317.8 DIP= 67.4 F10.7=180.2 DDD: 355 UT:19.0 SDE=-23.5

Date: 12/21, Time 00 L.T., SSN = 137, 40 N, 105 W

H/KM	ELECTRON DENSITY		TEMPERATURES				ION PERCENTAGE DENSITIES				
	NE/CM-3	NE/NMF2	TN/K	TI/K	TE/K	TE/TI	O+	H+	He+	O2+	NO+
60.0	0	-1.0000	-1	-1	-1	-1.00	-1	-1	-1	-1	-1
70.0	0	-1.0000	-1	-1	-1	-1.00	-1	-1	-1	-1	-1
80.0	1	0.0000	-1	-1	-1	-1.00	-1	-1	-1	-1	-1
90.0	472	0.0027	-1	-1	-1	-1.00	-1	-1	-1	-1	-1
100.0	3713	0.0215	-1	-1	-1	-1.00	0	0	0	16	84
110.0	3050	0.0176	-1	-1	-1	-1.00	0	0	0	22	78
120.0	1262	0.0073	355	355	355	1.00	0	0	0	29	71
130.0	733	0.0042	492	492	492	1.00	0	0	0	38	62
140.0	822	0.0048	598	598	598	1.00	1	0	0	42	58
150.0	1371	0.0079	681	681	698	1.03	2	0	0	39	59
160.0	2319	0.0134	746	746	762	1.02	7	0	0	34	59
170.0	3730	0.0216	796	796	806	1.01	20	0	0	29	51
180.0	4311	0.0249	835	835	847	1.01	43	0	0	20	37
190.0	5030	0.0291	865	865	887	1.02	65	0	0	10	25
200.0	5957	0.0344	889	889	926	1.04	78	0	0	4	18
210.0	7223	0.0417	908	908	966	1.06	85	0	0	1	14
220.0	9149	0.0529	922	922	1006	1.09	88	0	0	1	11
230.0	13645	0.0789	934	934	1046	1.12	90	0	0	0	10
240.0	27211	0.1573	943	943	1086	1.15	92	0	0	0	8
250.0	47377	0.2738	950	950	1125	1.18	94	0	0	0	6
260.0	73074	0.4224	955	955	1165	1.22	95	0	0	0	5
270.0	101301	0.5855	959	959	1205	1.26	97	0	0	0	3
280.0	128032	0.7400	963	963	1244	1.29	98	0	0	0	2
290.0	149644	0.8650	965	965	1282	1.33	99	0	0	0	1
300.0	164099	0.9485	968	968	1311	1.35	100	0	0	0	0
310.0	171344	0.9904	969	969	1323	1.37	100	0	0	0	0
320.0	173003	1.0000	970	970	1327	1.37	100	0	0	0	0
330.0	172709	0.9983	972	972	1329	1.37	100	0	0	0	0
340.0	171907	0.9937	972	972	1331	1.37	100	0	0	0	0
350.0	170610	0.9862	973	973	1332	1.37	100	0	0	0	0

I-URSI --B0Gul----------I----------I----------I

LAT/LON= 40.0/***** H= 350.0 RZ12=137.0 MMDD:1221 LT: 0.0 SZA=163.5

MLA/MLO= 48.9/317.8 DIP= 67.4 F10.7=180.2 DDD: 355 UT: 7.0 SDE=-23.5

Atmosphere

Date: 06/21, Time 12 L.T., SSN = 12, 40 N, 105 W

H/KM	NUMBER DENSITIES/CM-3			MASS DENSITY	TEMPERATURE/K	
	O	N2	O2	G*CM-3	TN	TEXO
60.0	2.892E+03	4.685E+15	1.256E+15	2.882E-07	298	862
70.0	3.035E+06	1.660E+15	4.443E+14	1.021E-07	223	862
80.0	4.929E+09	3.847E+14	1.023E+14	2.362E-08	180	862
90.0	1.881E+11	5.931E+13	1.534E+13	3.623E-09	169	862
100.0	2.860E+11	8.153E+12	1.899E+12	4.930E-10	193	862
110.0	1.485E+11	1.440E+12	2.603E+11	8.543E-11	243	862
120.0	5.975E+10	3.182E+11	4.130E+10	1.868E-11	354	862
130.0	2.854E+10	1.083E+11	1.111E+10	6.409E-12	489	862
140.0	1.661E+10	5.004E+10	4.496E+09	3.016E-12	588	862
150.0	1.074E+10	2.687E+10	2.215E+09	1.657E-12	660	862
160.0	7.413E+09	1.572E+10	1.211E+09	9.945E-13	713	862
170.0	5.342E+09	9.718E+09	7.035E+08	6.325E-13	752	862
180.0	3.966E+09	6.226E+09	4.252E+08	4.185E-13	781	862
190.0	3.009E+09	4.089E+09	2.640E+08	2.849E-13	802	862
200.0	2.319E+09	2.733E+09	1.671E+08	1.982E-13	818	862
210.0	1.810E+09	1.850E+09	1.072E+08	1.403E-13	829	862
220.0	1.426E+09	1.264E+09	6.948E+07	1.008E-13	838	862
230.0	1.131E+09	8.698E+08	4.537E+07	7.330E-14	844	862
240.0	9.031E+08	6.018E+08	2.981E+07	5.388E-14	849	862
250.0	7.245E+08	4.181E+08	1.967E+07	4.000E-14	852	862
260.0	5.835E+08	2.915E+08	1.303E+07	2.997E-14	855	862
270.0	4.715E+08	2.038E+08	8.660E+06	2.265E-14	857	862
280.0	3.821E+08	1.428E+08	5.769E+06	1.725E-14	858	862
290.0	3.103E+08	1.003E+08	3.852E+06	1.324E-14	859	862
300.0	2.526E+08	7.053E+07	2.577E+06	1.023E-14	860	862
310.0	2.021E+08	4.969E+07	1.727E+06	7.861E-15	860	862
320.0	1.655E+08	3.505E+07	1.159E+06	6.164E-15	861	862
330.0	1.357E+08	2.476E+07	7.791E+05	4.861E-15	861	862
340.0	1.113E+08	1.751E+07	5.245E+05	3.853E-15	861	862
350.0	9.139E+07	1.240E+07	3.535E+05	3.069E-15	862	862

LATI/LONG= 40.0/***** H= 350.0 F10.7 = 72.6 DAY:172 LT:12.0 AP= 5.0
MLAT/MLON= 48.9/317.8 F10.7M= 72.6 UT:19.0

Date: 06/21, Time 00 L.T., SSN = 12, 40 N, 105 W

H/KM	NUMBER DENSITIES/CM-3			MASS DENSITY	TEMPERATURE/K	
	O	N2	O2	G*CM-3	TN	TEXO
60.0	3.316E+03	5.599E+15	1.501E+15	3.444E-07	285	726
70.0	3.230E+06	1.853E+15	4.959E+14	1.139E-07	218	726
80.0	4.985E+09	4.110E+14	1.093E+14	2.523E-08	180	726
90.0	1.875E+11	6.296E+13	1.629E+13	3.844E-09	169	726
100.0	2.835E+11	8.681E+12	2.024E+12	5.242E-10	192	726
110.0	1.462E+11	1.523E+12	2.752E+11	9.000E-11	234	726
120.0	5.652E+10	3.199E+11	4.130E+10	1.866E-11	343	726
130.0	2.653E+10	1.066E+11	1.085E+10	6.258E-12	471	726
140.0	1.537E+10	4.879E+10	4.331E+09	2.914E-12	556	726
150.0	9.867E+09	2.583E+10	2.094E+09	1.578E-12	613	726
160.0	6.730E+09	1.479E+10	1.113E+09	9.272E-13	651	726
170.0	4.769E+09	8.879E+09	6.243E+08	5.735E-13	676	726
180.0	3.467E+09	5.486E+09	3.614E+08	3.669E-13	692	726
190.0	2.565E+09	3.454E+09	2.135E+08	2.405E-13	703	726
200.0	1.922E+09	2.202E+09	1.278E+08	1.606E-13	711	726
210.0	1.455E+09	1.416E+09	7.729E+07	1.089E-13	716	726
220.0	1.109E+09	9.165E+08	4.703E+07	7.479E-14	719	726
230.0	8.505E+08	5.957E+08	2.876E+07	5.200E-14	721	726
240.0	6.555E+08	3.885E+08	1.765E+07	3.656E-14	723	726
250.0	5.072E+08	2.541E+08	1.086E+07	2.598E-14	724	726
260.0	3.938E+08	1.665E+08	6.704E+06	1.866E-14	725	726
270.0	3.067E+08	1.094E+08	4.146E+06	1.353E-14	725	726
280.0	2.395E+08	7.193E+07	2.569E+06	9.904E-15	725	726
290.0	1.874E+08	4.739E+07	1.595E+06	7.316E-15	725	726
300.0	1.469E+08	3.126E+07	9.913E+05	5.450E-15	726	726
310.0	1.127E+08	2.065E+07	6.173E+05	4.022E-15	726	726
320.0	8.901E+07	1.366E+07	3.849E+05	3.049E-15	726	726
330.0	7.034E+07	9.051E+06	2.404E+05	2.326E-15	726	726
340.0	5.563E+07	6.003E+06	1.504E+05	1.785E-15	726	726
350.0	4.403E+07	3.986E+06	9.418E+04	1.377E-15	726	726

LATI/LONG= 40.0/***** H= 350.0 F10.7 = 72.6 DAY:172 LT: .0 AP= 5.0
MLAT/MLON= 48.9/317.8 F10.7M= 72.6 UT: 7.0

Date: 12/21, Time 12 L.T., SSN = 12, 40 N, 105 W

H/KM	NUMBER DENSITIES/CM-3			MASS DENSITY	TEMPERATURE/K	
	O	N2	O2	G*CM-3	TN	TEXO
60.0	3.543E+04	4.784E+16	1.283E+16	2.942E-06	52	745
70.0	1.161E+06	5.140E+14	1.376E+14	3.160E-08	306	745
80.0	3.428E+09	2.101E+14	5.592E+13	1.289E-08	239	745
90.0	2.204E+11	5.286E+13	1.377E+13	3.231E-09	192	745
100.0	4.420E+11	9.331E+12	2.233E+12	5.696E-10	190	745
110.0	2.315E+11	1.567E+12	3.018E+11	9.565E-11	226	745
120.0	9.163E+10	3.249E+11	4.751E+10	2.014E-11	345	745
130.0	4.741E+10	1.129E+11	1.348E+10	7.242E-12	443	745
140.0	2.829E+10	5.003E+10	5.258E+09	3.362E-12	516	745
150.0	1.841E+10	2.530E+10	2.425E+09	1.796E-12	572	745
160.0	1.269E+10	1.386E+10	1.229E+09	1.048E-12	614	745
170.0	9.084E+09	8.012E+09	6.616E+08	6.499E-13	646	745
180.0	6.682E+09	4.803E+09	3.706E+08	4.212E-13	670	745
190.0	5.009E+09	2.954E+09	2.135E+08	2.824E-13	688	745
200.0	3.807E+09	1.852E+09	1.255E+08	1.945E-13	702	745
210.0	2.923E+09	1.177E+09	7.496E+07	1.369E-13	712	745
220.0	2.262E+09	7.560E+08	4.528E+07	9.809E-14	720	745
230.0	1.760E+09	4.897E+08	2.759E+07	7.138E-14	726	745
240.0	1.375E+09	3.192E+08	1.694E+07	5.262E-14	731	745
250.0	1.079E+09	2.091E+08	1.045E+07	3.923E-14	734	745
260.0	8.484E+08	1.376E+08	6.481E+06	2.953E-14	737	745
270.0	6.688E+08	9.082E+07	4.033E+06	2.242E-14	739	745
280.0	5.281E+08	6.013E+07	2.518E+06	1.715E-14	740	745
290.0	4.177E+08	3.991E+07	1.577E+06	1.320E-14	742	745
300.0	3.308E+08	2.655E+07	9.896E+05	1.022E-14	742	745
310.0	2.627E+08	1.769E+07	6.225E+05	7.966E-15	743	745
320.0	2.085E+08	1.181E+07	3.923E+05	6.226E-15	744	745
330.0	1.656E+08	7.898E+06	2.477E+05	4.886E-15	744	745
340.0	1.317E+08	5.290E+06	1.567E+05	3.849E-15	744	745
350.0	1.048E+08	3.548E+06	9.925E+04	3.042E-15	745	745

LATI/LONG= 40.0/***** H= 350.0 F10.7 = 72.6 DAY:355 LT:12.0 AP= 5.0
MLAT/MLON= 48.9/317.8 F10.7M= 72.6 UT:19.0

Date: 12/21, Time 00 L.T., SSN = 12, 40 N, 105 W

H/KM	NUMBER DENSITIES/CM-3			MASS DENSITY	TEMPERATURE/K	
	O	N2	O2	G*CM-3	TN	TEXO
60.0	1.910E+04	2.644E+16	7.089E+15	1.626E-06	65	664
70.0	1.175E+06	5.357E+14	1.434E+14	3.293E-08	314	664
80.0	3.509E+09	2.223E+14	5.917E+13	1.364E-08	234	664
90.0	2.167E+11	5.395E+13	1.405E+13	3.298E-09	191	664
100.0	4.318E+11	9.510E+12	2.277E+12	5.801E-10	190	664
110.0	2.272E+11	1.608E+12	3.096E+11	9.787E-11	222	664
120.0	8.895E+10	3.267E+11	4.754E+10	2.015E-11	334	664
130.0	4.508E+10	1.104E+11	1.308E+10	7.043E-12	429	664
140.0	2.662E+10	4.813E+10	4.998E+09	3.215E-12	496	664
150.0	1.716E+10	2.393E+10	2.257E+09	1.690E-12	544	664
160.0	1.169E+10	1.285E+10	1.117E+09	9.682E-13	578	664
170.0	8.253E+09	7.250E+09	5.839E+08	5.880E-13	602	664
180.0	5.972E+09	4.225E+09	3.163E+08	3.724E-13	620	664
190.0	4.395E+09	2.518E+09	1.755E+08	2.436E-13	632	664
200.0	3.273E+09	1.524E+09	9.910E+07	1.634E-13	641	664
210.0	2.458E+09	9.327E+08	5.664E+07	1.120E-13	647	664
220.0	1.857E+09	5.757E+08	3.266E+07	7.812E-14	652	664
230.0	1.410E+09	3.575E+08	1.896E+07	5.534E-14	655	664
240.0	1.074E+09	2.231E+08	1.107E+07	3.972E-14	658	664
250.0	8.210E+08	1.398E+08	6.489E+06	2.884E-14	659	664
260.0	6.286E+08	8.785E+07	3.817E+06	2.115E-14	660	664
270.0	4.823E+08	5.536E+07	2.252E+06	1.565E-14	661	664
280.0	3.705E+08	3.496E+07	1.332E+06	1.167E-14	662	664
290.0	2.851E+08	2.212E+07	7.898E+05	8.757E-15	662	664
300.0	2.196E+08	1.403E+07	4.692E+05	6.613E-15	663	664
310.0	1.691E+08	8.907E+06	2.792E+05	5.014E-15	663	664
320.0	1.306E+08	5.665E+06	1.665E+05	3.825E-15	663	664
330.0	1.009E+08	3.609E+06	9.946E+04	2.931E-15	663	664
340.0	7.804E+07	2.302E+06	5.950E+04	2.254E-15	663	664
350.0	6.041E+07	1.471E+06	3.566E+04	1.740E-15	663	664

LATI/LONG= 40.0/***** H= 350.0 F10.7 = 72.6 DAY:355 LT: .0 AP= 5.0
MLAT/MLON= 48.9/317.8 F10.7M= 72.6 UT: 7.0

Date: 06/21, Time 12 L.T., SSN = 137, 40 N, 105 W

H/KM	NUMBER DENSITIES/CM-3			MASS DENSITY	TEMPERATURE/K	
	O	N2	O2	G*CM-3	TN	TEXO
60.0	1.559E+03	2.325E+15	6.231E+14	1.430E-07	458	1330
70.0	2.830E+06	1.407E+15	3.763E+14	8.650E-08	247	1330
80.0	5.544E+09	3.881E+14	1.029E+14	2.381E-08	191	1330
90.0	2.383E+11	6.651E+13	1.706E+13	4.055E-09	168	1330
100.0	3.624E+11	9.002E+12	2.041E+12	5.425E-10	190	1330
110.0	1.854E+11	1.541E+12	2.584E+11	9.102E-11	245	1330
120.0	7.307E+10	3.315E+11	3.751E+10	1.945E-11	377	1330
130.0	3.455E+10	1.130E+11	9.778E+09	6.721E-12	557	1330
140.0	2.045E+10	5.416E+10	4.081E+09	3.289E-12	703	1330
150.0	1.360E+10	3.064E+10	2.135E+09	1.905E-12	821	1330
160.0	9.737E+09	1.909E+10	1.258E+09	1.217E-12	916	1330
170.0	7.321E+09	1.268E+10	7.966E+08	8.288E-13	993	1330
180.0	5.698E+09	8.790E+09	5.288E+08	5.904E-13	1056	1330
190.0	4.549E+09	6.286E+09	3.630E+08	4.345E-13	1107	1330
200.0	3.703E+09	4.601E+09	2.555E+08	3.277E-13	1148	1330
210.0	3.059E+09	3.426E+09	1.833E+08	2.520E-13	1182	1330
220.0	2.556E+09	2.586E+09	1.334E+08	1.968E-13	1209	1330
230.0	2.156E+09	1.973E+09	9.814E+07	1.557E-13	1231	1330
240.0	1.833E+09	1.518E+09	7.289E+07	1.244E-13	1250	1330
250.0	1.567E+09	1.176E+09	5.453E+07	1.003E-13	1264	1330
260.0	1.347E+09	9.163E+08	4.105E+07	8.153E-14	1276	1330
270.0	1.162E+09	7.170E+08	3.105E+07	6.672E-14	1286	1330
280.0	1.006E+09	5.633E+08	2.359E+07	5.492E-14	1294	1330
290.0	8.739E+08	4.439E+08	1.798E+07	4.546E-14	1301	1330
300.0	7.607E+08	3.507E+08	1.374E+07	3.782E-14	1306	1330
310.0	6.571E+08	2.778E+08	1.053E+07	3.144E-14	1310	1330
320.0	5.751E+08	2.204E+08	8.090E+06	2.641E-14	1314	1330
330.0	5.039E+08	1.752E+08	6.226E+06	2.226E-14	1317	1330
340.0	4.420E+08	1.395E+08	4.799E+06	1.884E-14	1319	1330
350.0	3.881E+08	1.112E+08	3.705E+06	1.599E-14	1321	1330

LATI/LONG= 40.0/***** H= 350.0 F10.7 =180.2 DAY:172 LT:12.0 AP= 5.0
MLAT/MLON= 48.9/317.8 F10.7M=180.2 UT:19.0

Date: 06/21, Time 00 L.T., SSN = 137, 40 N, 105 W

H/KM	NUMBER DENSITIES/CM-3			MASS DENSITY	TEMPERATURE/K	
	O	N2	O2	G*CM-3	TN	TEXO
60.0	1.696E+03	2.653E+15	7.112E+14	1.632E-07	457	1071
70.0	3.028E+06	1.591E+15	4.254E+14	9.777E-08	238	1071
80.0	5.552E+09	4.139E+14	1.098E+14	2.539E-08	189	1071
90.0	2.336E+11	7.005E+13	1.798E+13	4.269E-09	168	1071
100.0	3.529E+11	9.512E+12	2.158E+12	5.722E-10	189	1071
110.0	1.796E+11	1.623E+12	2.722E+11	9.543E-11	237	1071
120.0	6.808E+10	3.332E+11	3.752E+10	1.939E-11	366	1071
130.0	3.160E+10	1.115E+11	9.572E+09	6.555E-12	540	1071
140.0	1.861E+10	5.316E+10	3.965E+09	3.185E-12	670	1071
150.0	1.233E+10	2.990E+10	2.055E+09	1.831E-12	768	1071
160.0	8.771E+09	1.844E+10	1.194E+09	1.156E-12	842	1071
170.0	6.535E+09	1.207E+10	7.414E+08	7.757E-13	898	1071
180.0	5.028E+09	8.205E+09	4.802E+08	5.418E-13	940	1071
190.0	3.957E+09	5.729E+09	3.201E+08	3.896E-13	972	1071
200.0	3.168E+09	4.077E+09	2.178E+08	2.862E-13	996	1071
210.0	2.569E+09	2.942E+09	1.504E+08	2.139E-13	1014	1071
220.0	2.104E+09	2.144E+09	1.050E+08	1.619E-13	1028	1071
230.0	1.736E+09	1.576E+09	7.395E+07	1.239E-13	1038	1071
240.0	1.441E+09	1.165E+09	5.240E+07	9.577E-14	1046	1071
250.0	1.203E+09	8.648E+08	3.733E+07	7.462E-14	1052	1071
260.0	1.008E+09	6.446E+08	2.669E+07	5.856E-14	1056	1071
270.0	8.469E+08	4.819E+08	1.915E+07	4.627E-14	1060	1071
280.0	7.138E+08	3.612E+08	1.378E+07	3.678E-14	1063	1071
290.0	6.029E+08	2.713E+08	9.937E+06	2.941E-14	1065	1071
300.0	5.103E+08	2.041E+08	7.180E+06	2.364E-14	1066	1071
310.0	4.262E+08	1.538E+08	5.197E+06	1.894E-14	1067	1071
320.0	3.627E+08	1.160E+08	3.767E+06	1.539E-14	1068	1071
330.0	3.089E+08	8.766E+07	2.734E+06	1.257E-14	1069	1071
340.0	2.633E+08	6.630E+07	1.987E+06	1.031E-14	1069	1071
350.0	2.246E+08	5.020E+07	1.446E+06	8.483E-15	1070	1071

LATI/LONG= 40.0/***** H= 350.0 F10.7 =180.2 DAY:172 LT: .0 AP= 5.0
MLAT/MLON= 48.9/317.8 F10.7M=180.2 UT: 7.0

Date: 12/21, Time 12 L.T., SSN = 137, 40 N, 105 W

H/KM	NUMBER DENSITIES/CM-3			MASS DENSITY	TEMPERATURE/K	
	O	N2	O2	G*CM-3	TN	TEXO
60.0	5.496E+06	6.948E+18	1.863E+18	4.273E-04	20	1135
70.0	1.995E+06	8.184E+14	2.189E+14	5.029E-08	181	1135
80.0	2.912E+09	1.634E+14	4.338E+13	1.002E-08	291	1135
90.0	2.597E+11	5.642E+13	1.457E+13	3.443E-09	198	1135
100.0	5.533E+11	1.046E+13	2.439E+12	6.368E-10	189	1135
110.0	2.916E+11	1.739E+12	3.107E+11	1.057E-10	223	1135
120.0	1.093E+11	3.384E+11	4.312E+10	2.100E-11	368	1135
130.0	5.578E+10	1.182E+11	1.191E+10	7.628E-12	509	1135
140.0	3.400E+10	5.508E+10	4.873E+09	3.729E-12	623	1135
150.0	2.296E+10	2.989E+10	2.437E+09	2.132E-12	716	1135
160.0	1.656E+10	1.779E+10	1.363E+09	1.341E-12	792	1135
170.0	1.249E+10	1.127E+10	8.170E+08	9.010E-13	854	1135
180.0	9.727E+09	7.458E+09	5.137E+08	6.341E-13	905	1135
190.0	7.749E+09	5.092E+09	3.343E+08	4.620E-13	946	1135
200.0	6.278E+09	3.560E+09	2.233E+08	3.457E-13	980	1135
210.0	5.150E+09	2.535E+09	1.521E+08	2.642E-13	1008	1135
220.0	4.266E+09	1.831E+09	1.052E+08	2.053E-13	1030	1135
230.0	3.561E+09	1.337E+09	7.366E+07	1.618E-13	1049	1135
240.0	2.989E+09	9.858E+08	5.209E+07	1.290E-13	1064	1135
250.0	2.521E+09	7.320E+08	3.713E+07	1.039E-13	1077	1135
260.0	2.134E+09	5.468E+08	2.664E+07	8.431E-14	1087	1135
270.0	1.811E+09	4.106E+08	1.922E+07	6.892E-14	1096	1135
280.0	1.542E+09	3.096E+08	1.393E+07	5.669E-14	1102	1135
290.0	1.315E+09	2.342E+08	1.014E+07	4.689E-14	1108	1135
300.0	1.124E+09	1.778E+08	7.402E+06	3.897E-14	1113	1135
310.0	9.695E+08	1.353E+08	5.419E+06	3.274E-14	1117	1135
320.0	8.295E+08	1.032E+08	3.978E+06	2.740E-14	1120	1135
330.0	7.106E+08	7.884E+07	2.926E+06	2.302E-14	1123	1135
340.0	6.095E+08	6.036E+07	2.157E+06	1.939E-14	1125	1135
350.0	5.233E+08	4.628E+07	1.593E+06	1.639E-14	1126	1135

LATI/LONG= 40.0/***** H= 350.0 F10.7 =180.2 DAY:355 LT:12.0 AP= 5.0
MLAT/MLON= 48.9/317.8 F10.7M=180.2 UT:19.0

Date: 12/21, Time 00 L.T., SSN = 137, 40 N, 105 W

H/KM	NUMBER DENSITIES/CM-3			MASS DENSITY	TEMPERATURE/K	
	O	N2	O2	G*CM-3	TN	TEXO
60.0	9.421E+05	1.224E+18	3.281E+17	7.526E-05	26	980
70.0	1.603E+06	6.786E+14	1.815E+14	4.170E-08	217	980
80.0	3.035E+09	1.765E+14	4.688E+13	1.083E-08	281	980
90.0	2.545E+11	5.759E+13	1.488E+13	3.514E-09	197	980
100.0	5.368E+11	1.063E+13	2.477E+12	6.460E-10	189	980
110.0	2.839E+11	1.778E+12	3.176E+11	1.078E-10	220	980
120.0	1.054E+11	3.402E+11	4.316E+10	2.099E-11	357	980
130.0	5.276E+10	1.160E+11	1.160E+10	7.429E-12	494	980
140.0	3.190E+10	5.346E+10	4.680E+09	3.587E-12	601	980
150.0	2.140E+10	2.873E+10	2.311E+09	2.029E-12	684	980
160.0	1.533E+10	1.690E+10	1.273E+09	1.262E-12	748	980
170.0	1.148E+10	1.056E+10	7.500E+08	8.368E-13	799	980
180.0	8.851E+09	6.868E+09	4.620E+08	5.800E-13	838	980
190.0	6.973E+09	4.598E+09	2.936E+08	4.155E-13	869	980
200.0	5.578E+09	3.144E+09	1.909E+08	3.053E-13	893	980
210.0	4.513E+09	2.184E+09	1.263E+08	2.289E-13	911	980
220.0	3.682E+09	1.536E+09	8.466E+07	1.744E-13	926	980
230.0	3.023E+09	1.090E+09	5.731E+07	1.346E-13	938	980
240.0	2.494E+09	7.794E+08	3.911E+07	1.051E-13	947	980
250.0	2.066E+09	5.605E+08	2.686E+07	8.279E-14	954	980
260.0	1.716E+09	4.050E+08	1.854E+07	6.577E-14	959	980
270.0	1.429E+09	2.938E+08	1.286E+07	5.262E-14	964	980
280.0	1.192E+09	2.138E+08	8.945E+06	4.236E-14	967	980
290.0	9.958E+08	1.560E+08	6.242E+06	3.428E-14	970	980
300.0	8.331E+08	1.141E+08	4.367E+06	2.788E-14	972	980
310.0	7.017E+08	8.359E+07	3.062E+06	2.288E-14	973	980
320.0	5.877E+08	6.137E+07	2.151E+06	1.875E-14	975	980
330.0	4.928E+08	4.512E+07	1.514E+06	1.542E-14	976	980
340.0	4.136E+08	3.322E+07	1.067E+06	1.272E-14	977	980
350.0	3.474E+08	2.449E+07	7.532E+05	1.053E-14	977	980

LATI/LONG= 40.0/***** H= 350.0 F10.7 =180.2 DAY:355 LT: .0 AP= 5.0
MLAT/MLON= 48.9/317.8 F10.7M=180.2 UT: 7.0